# Astrofisica Nucleare e Subnucleare

## “keV” Astrophysics

# Detector Project



## Definition of Terms

- **Effective Area:**

  $A_{eff}$

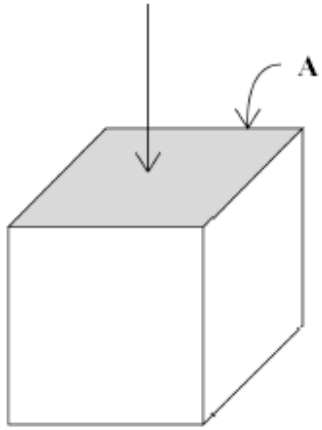


Area at normal incidence times detection efficiency.

- **Energy Resolution:**

  $E_R$

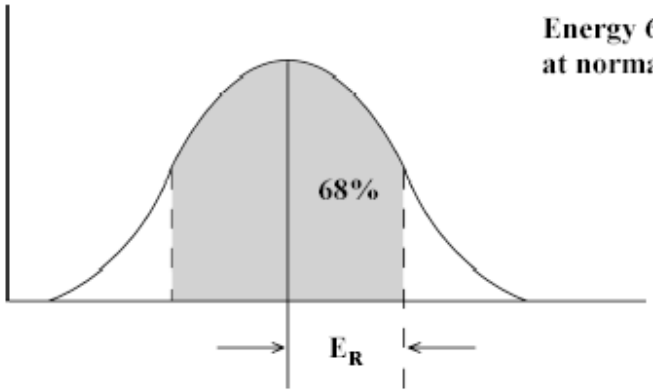


Energy 68% spread at normal incidence.

# Detector Project



## Definition of Terms

- **Angular Resolution:**

  $\Theta_R$

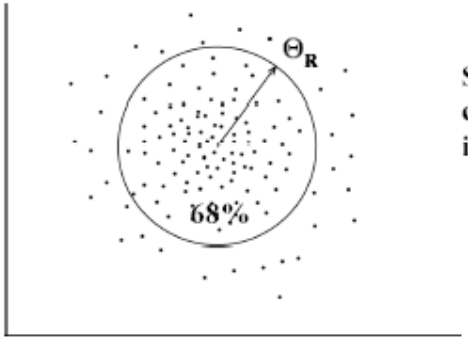


Space angle for 68% containment at normal incidence.

- **Field of View:**

  FOV

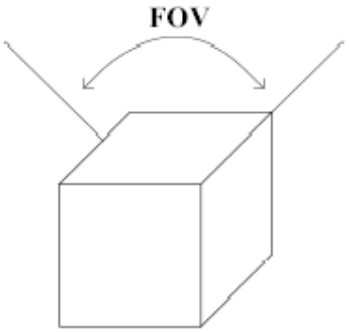


Integral effective area over solid angle divided by peak effective area.

- **Sensitivity:**

Flux of weakest source that can be detected at 5 sigma significance.

# Outline

- keV astrophysics
  - Principles of detection – Xray imaging, spectroscopy, calorimetry, polarimetry
  - Chandra, XMM
  - ROSAT, RXTE, BeppoSAX
  - Suzaku, NuSTAR, Astro-H, MAXI, Nicer, ASTROSAT, HMXT
  - eROSITA, IXPE, XIPE, LOFT, eXTP, Athena

# Nobel prize 2002 – R.Giacconi

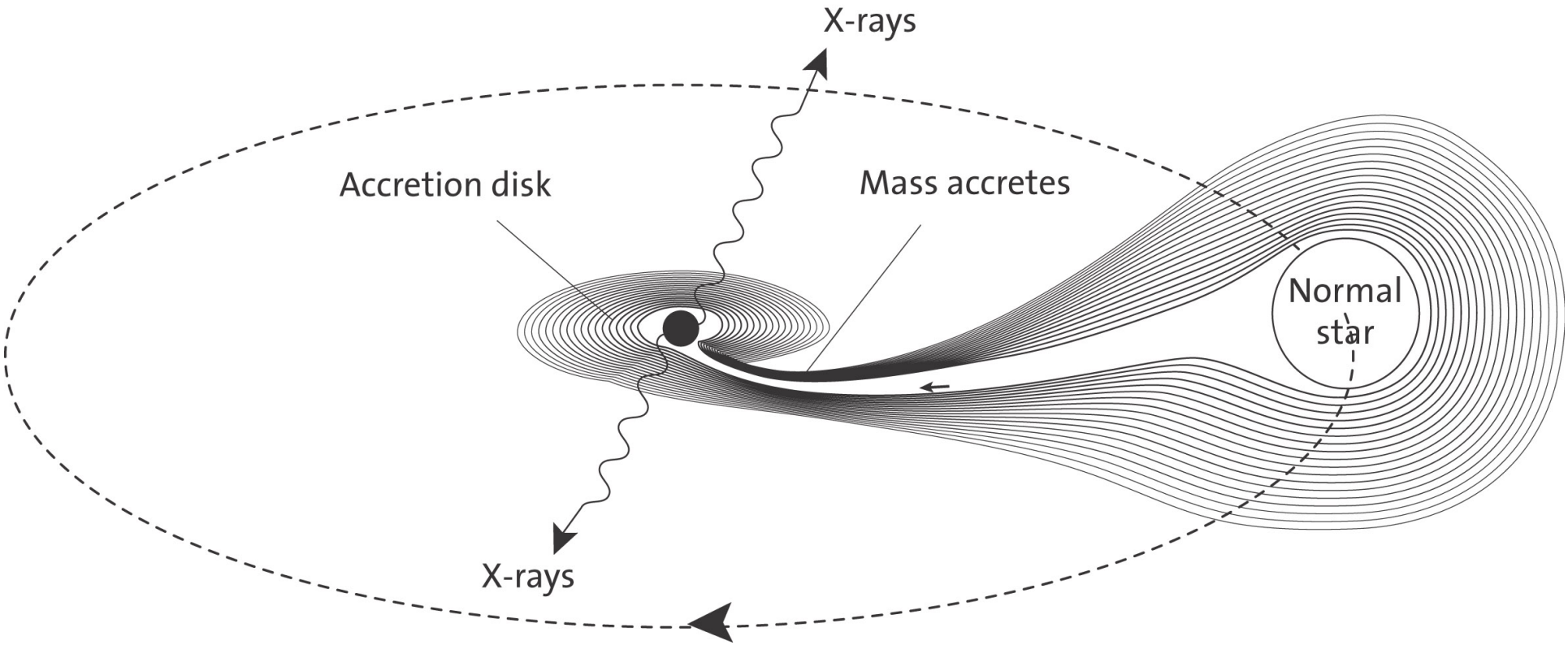


“ … for pioneering contributions to astrophysics,
which have led to the discovery of cosmic X-ray sources”

# Useful reference

## Cambridge University Press

## Handbook of Space Astronomy and Astrophysics

Martin V. Zombeck's **Handbook of Space Astronomy & Astrophysics, 2nd edition** is on-line at no cost. Published by Cambridge University Press, this handbook has become an essential reference for space astronomy and astrophysics. The complete 2nd edition (Copyright Cambridge University Press, 1982, 1990) is now available at your electronic desktop.

A 3rd edition of the Handbook of Space Astronomy & Astrophysics has been published. Fully updated, enlarged (nearly double the number of pages of the Second Edition) and including data from space-based observations, this 3rd edition is a comprehensive compilation of the facts and figures relevant to astronomy and astrophysics. As well as a

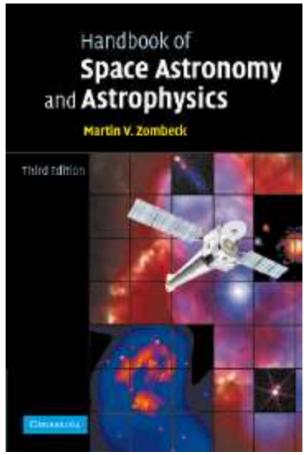


**Third Edition by Martin V. Zombeck**

**On-line Version of the 2nd Edition**

**Note:** All chapters now have links to related WWW resources containing extensive tabulations, images, interactive programs, etc.. Look for the link at the top of the table of contents for the given chapter.

**Citation form:** Zombeck, M. V., *Handbook of Astronomy and Astrophysics*, Cambridge, UK: Cambridge University Press.

- Table of Contents
- Index
- Links
- Help

http://ads.harvard.edu/books/hsaa

# Exercise #1

- Look at Chandra and XMM web site and find one of the Scientific Topics of your interest
- Find information on the currently operating and future satellites

  (Hitomi (?), IXPE, XIPE, LOFT/exTP,

  NICER, ASTROSAT, HMXT, eROSITA)

# *X-ray astronomical optics history in pills (I)*

- 1895: Roentgen discovers “X-rays”
- 1948: First succesful focalization of an X-ray beam by a total-reflection optics (Baez)
- 1952: H. Wolter proposes the use of two-reflection optics based on conics for X-ray microscopy
- 1960: R. Giacconi and B. Rossi propose the use of grazing incidence optics for X-ray telescopes
- 1962: discovery by Giacconi et al. of Sco-X1, the first extra-solar X-ray source
- 1963: Giacconi and Rossi fly the first (small) Wolter I optics to take images of Sun in X-rays
- 1965: second flight of a Wolter I focusing optics (Giacconi + Lindslay)
- 1970: *Uhuru*, the first satellite for X-ray astronomy (noX-ray optics)
- 1973: SKYLAB carry onboard two small X-ray optics for the study of the Sun
- 1978: *Einstein*, the first satellite with optics entirely dedicated to X-rays

# *X-ray astronomical optics history in pills (II)*

- 1983: *EXOSAT* operated (first European mission with X-ray optics aboard)
- 1990: *ROSAT*, first All Sky Survey in X-rays by means of a focusing telescope with high imaging capabilities
- 1993: *ASCA*, a multi-module focusing telescope with enhanced effective area for spectroscopic purposes
- 1996: *BeppoSAX*, a broad-band satellite with Ni electroformed optics
- 1999: launch of *Chandra*, the X-ray telescope with best angular resolution, and XMM-*Newton*, the X-ray telescope with most effective area
- 2004: launch of the *Swift* satellite devoted to the GRBs investigation (with aboard XRT)
- 2005: launch of *Suzaku* with high throughput optics for enhanced spectroscopy studies with bolometers
- 2012: launch of *NuSTAR* (with the first X-ray focusing imaging instrument)
- 2016: launch of *Astro-H/Hitomi* (Japanese mission including a calorimeter)

# Photon interactions

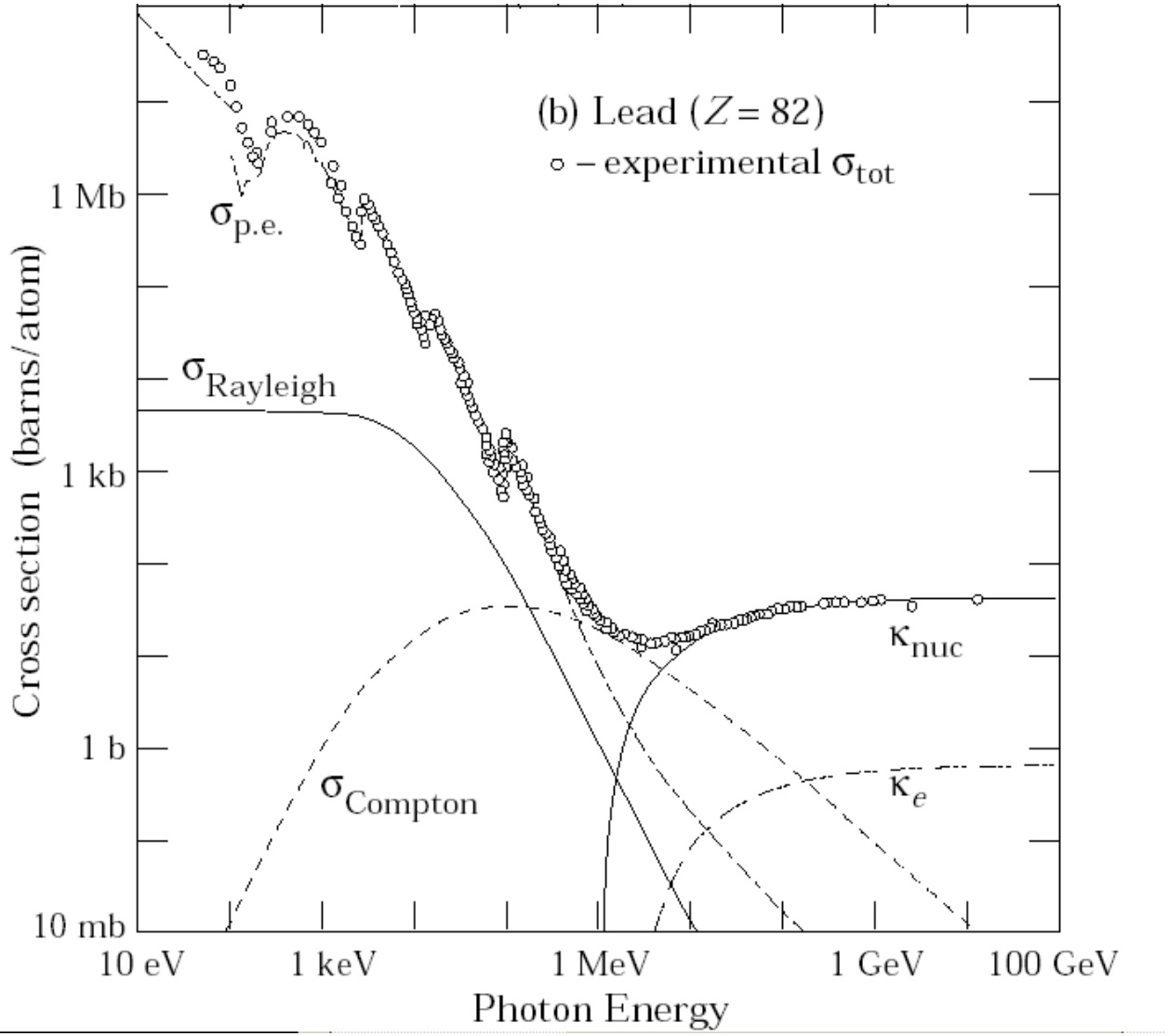

# Z vs E

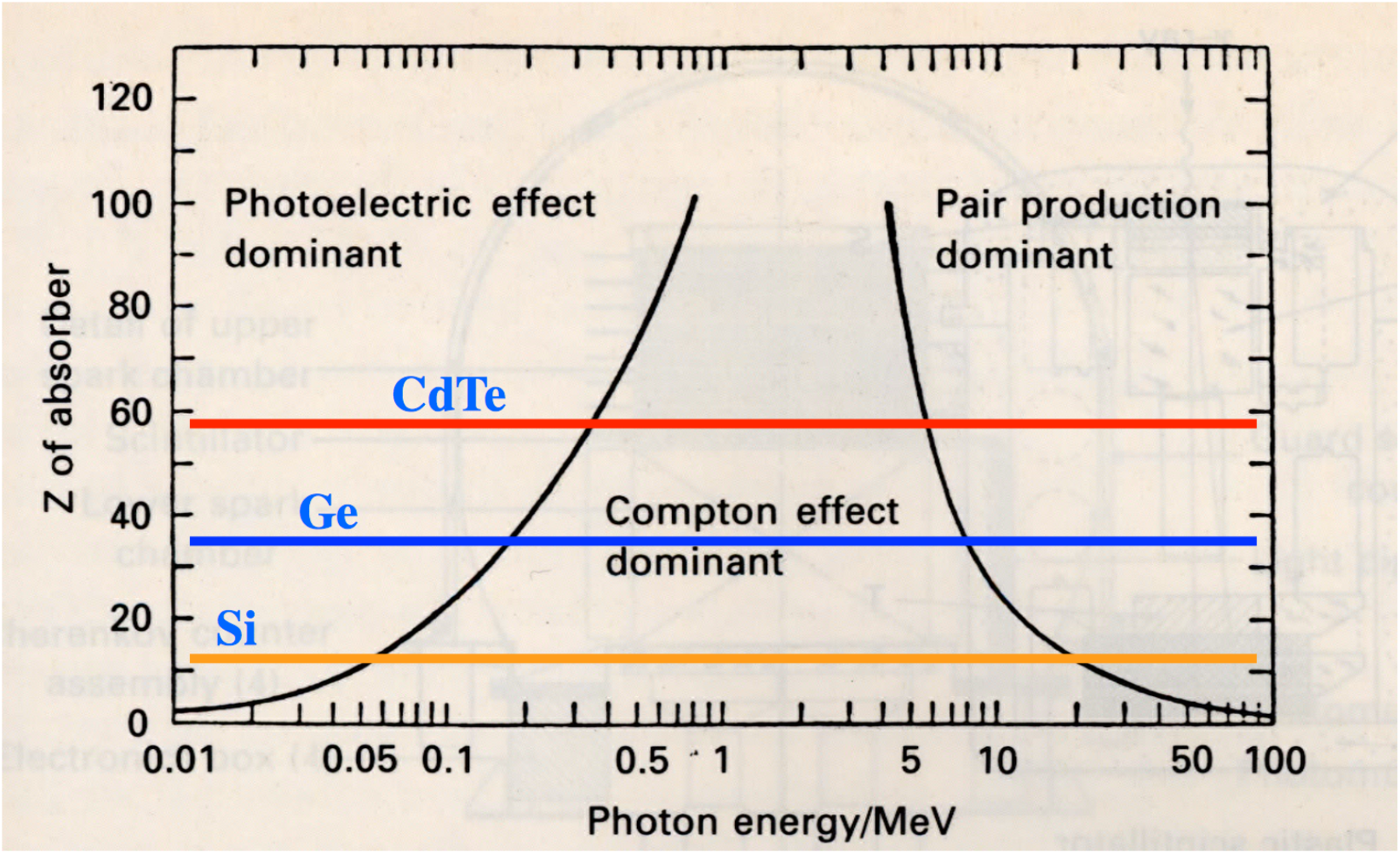
120
100
80
60
40
20
0
Z of absorber
Photoelectric effect
dominant
Pair production
dominant
CdTe
Ge
Compton effect
dominant
Si
0.01
0.05
0.1
0.5
1
5
10
50
100
Photon energy/MeV

# Strumentazioni per l'astrofisica

(prima parte)

## Rivelazione di raggi X/γ in condizioni astronomiche

**partly adapted from G. Malaguti's Lessons**

*Istituto Nazionale di Astrofisica (INAF) IASF-Bologna*

# Telescopi in banda X e γ

**Incidenza radente** (E<20 keV, presto anche ad energie maggiori) – configurazione di tipo Wolter I

**E≈20-100 keV**: collimatori, coded masks
**E≈0.2-10 MeV**: Compton Telescopes
**E>10 MeV**: Pair Telescopes (tracking chambers)
(gia' discussi)

# Telescopi per astronomia γ vs Energia

## Detection of Gamma Radiation

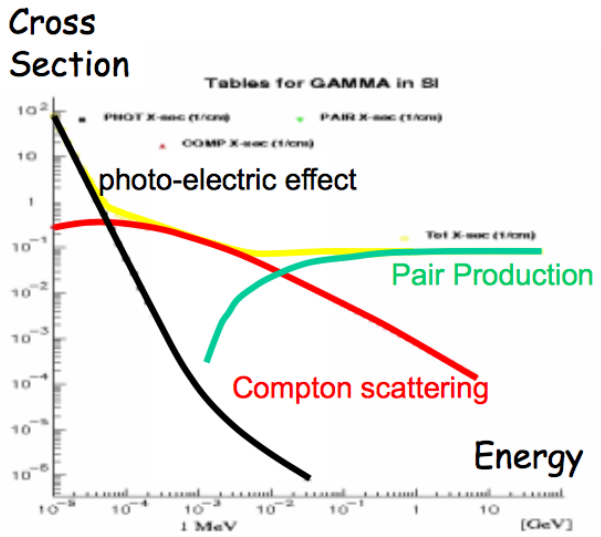


Photoeffect(< 100 keV)

Photons effectively blocked and stopped

Telescopes:

Collimators
Coded Mask Systems

Compton Scattering (0.2-10 MeV)
Photon Crossection Minimum
Scattered photons with long range
Telescope:
Compton Camera Coincidence System

Pair Creation (> 10 MeV)
Photons completely converted to $e^+e^-$

Telescope:
Tracking chambers to visualize the pairs

# Scanning with Slat Collimators

- Imaging the sky with non-imaging X-ray instruments as a goal
- Linear scanning means position is determined in one direction
- At least a second scanning, preferentially in the direction perpendicular to the previous one
- First all-sky survey in X-rays by Uhuru (1970-72): 2 prop. counters with metal collimators (0.5°×5°, 5°×5° FWHM )

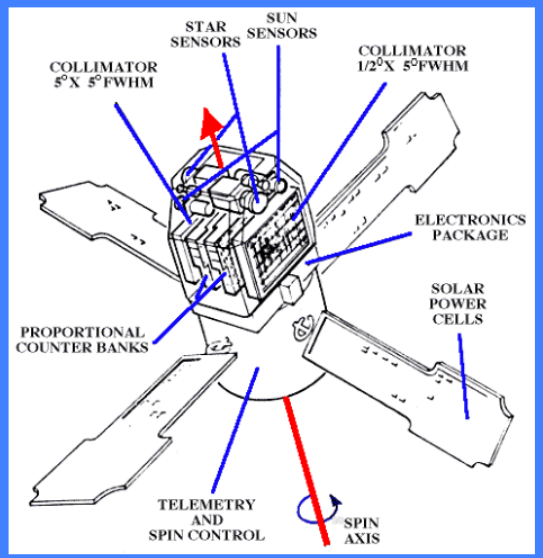


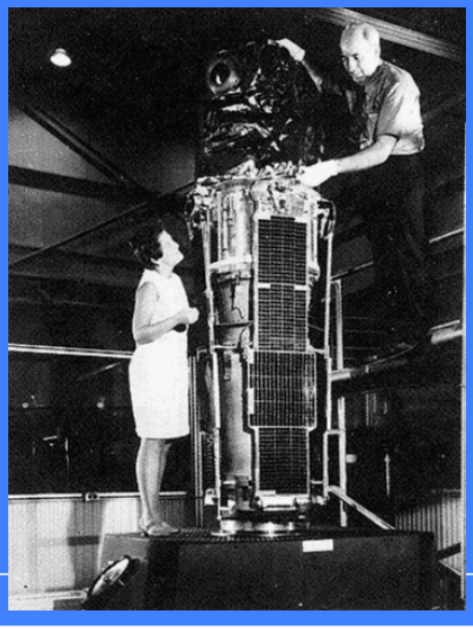

# Scanning Grid Collimators

- **Two or more plane ("grid" of absorbing rods) collimators to improve angular resolution**

- **Higher resolution with three or more grids (e.g., 4 in HEAO-1 A-3 experiment)**

- **Two-dimensional measurements need scans in two or more directions**

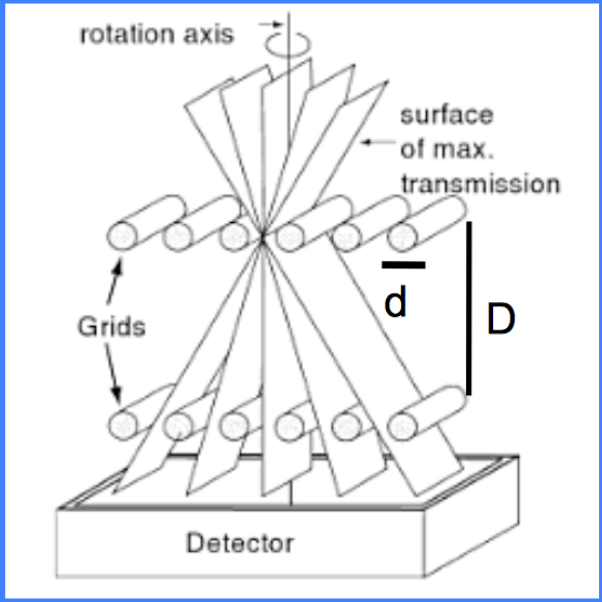


Double-grid collimator
Transmission Function of triangular shape
Angular resolution: d/D

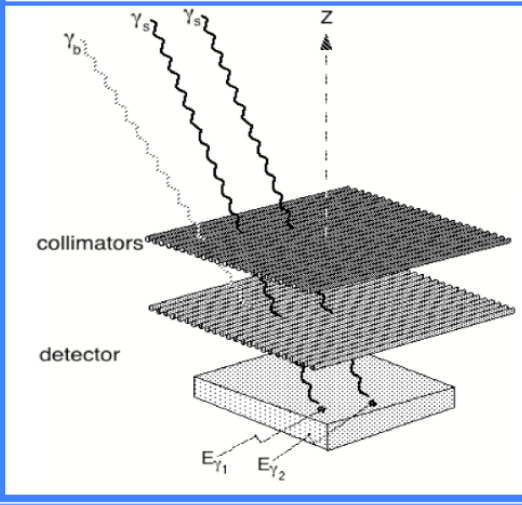


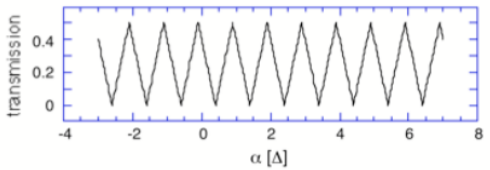


Modulation curve

# Sensibilità - 1

- **Sensibilità = flusso minimo rivelabile**
  - **Emissione nel continuo: fotoni $cm^{-2}$ $s^{-1}$ $keV^{-1}$**
  - **Emissione di righe: fotoni $cm^{-2}$ $s^{-1}$**
- **$C_S$ = Tasso di conteggi di sorgente**
- **$C_{Bkg}$ = Tasso di conteggi di fondo**

**assumendo una statistica poissoniana**

$$SNR = n_\sigma = \frac{C_S}{\sqrt{C_S + C_{Bkg}}}$$

**In realta' quello che si misura e' (S+B)-B in un dato intervallo di tempo**

$$S = (S+B) - B \longrightarrow \sigma_S^2 = \sigma_{S+B}^2 + \sigma_B^2 =$$

$$= (\sqrt{(S+B)})^2 + (\sqrt{B})^2 = S + B + B = S + 2B$$

$$SNR = S/\sigma_S = S/\sqrt{(S+2B)}$$

# Sensibilità – 2 – "basic" dependencies

$S = \varepsilon\ A\ T\ \Delta E\ F_{src}$

$B = \ A\ T\ \Delta E\ F_{bkg}$

ε=efficienza di rivelazione fotoni della sorgente
A=area efficace
T=tempo di esposizione
ΔE=banda energetica
$F_{src}$=flusso della sorgente
$F_{bkg}$=fondo strumentale

$B << \varepsilon F_{src}$

$$SNR = \frac{S}{\sqrt{S + 2B}} \approx \sqrt{S} \propto \sqrt{F_{src} T}$$

the source dominates the signal

$B >> \varepsilon F_{src}$

$$SNR = \frac{S}{\sqrt{S + 2B}} \approx S / \sqrt{2B} \propto \sqrt{T} (F_{src} / \sqrt{2F_{bkg}})$$

Backg-dominated obsn.

$$\mathrm{SNR} = n_\sigma \approx \frac{\varepsilon \cdot \mathrm{A} \cdot \mathrm{T} \cdot \Delta\mathrm{E} \cdot \mathrm{F}}{\sqrt{\mathrm{A} \cdot \mathrm{T} \cdot \Delta\mathrm{E} \cdot \mathrm{B}}} \rightarrow F_{Min} = \frac{n_\sigma}{\varepsilon} \sqrt{\frac{B}{\mathrm{A} \cdot \mathrm{T} \cdot \Delta\mathrm{E}}}$$

to give an idea of the main dependencies of the limiting flux (sensitivity)

In the "real world", the background is not only instrumental but also cosmic

S=source flux density [counts/m$^2$ s]
A=area of the detector
Ω=solid angle subtended by the beam of the telescope on the sky
$B_1$=instrumental (particle) background [counts/s]
$B_2$=cosmic background (XRB) [phot/m$^2$ s ster]
T=exposure time
**SOURCE**=S×A×T (photons related to the source)
**BACKGROUND**=$B_1$×T + $B_2$×A×Ω×T (photons related to the backgrounds)

$$N = \sqrt{(B_1 + B_2 A\Omega) \times T}$$

$$S/N = \frac{SAT}{\sqrt{(B_1 + B_2 A\Omega) \times T}} = \frac{SA^{1/2}T^{1/2}}{\sqrt{\left(\frac{B_1}{A}\right) + \Omega B_2}}$$

$$S/N = 5 \Rightarrow S_{\min} = 5\sqrt{\frac{B_1/A + \Omega B_2}{AT}}$$

# Focalizzazione vs collimazione

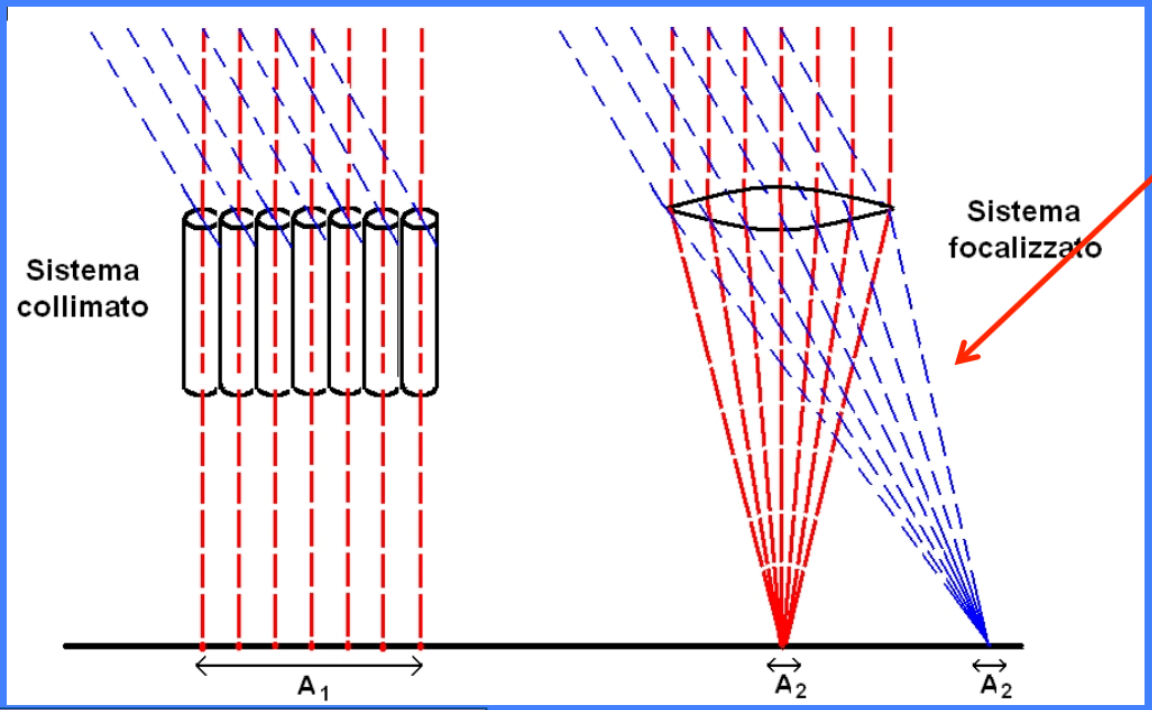


Proper imaging of X-rays below 20-40 keV

$$F_{\min} \approx n_\sigma \frac{\sqrt{2B}}{\sqrt{A_{\det} T_{\text{int}} \Delta E}}$$

$A_d$= PSF projected on the focal plane

$$F_{\min} \approx n_\sigma \frac{\sqrt{B A_d}}{A_{eff} \sqrt{T_{\text{int}} \Delta E}}$$

**Sistema collimato**: limita la regione di cielo da cui puo' provenire un segnale, (quindi limita il background), non incrementandone la "densita"

**Sistema focalizzato**: fa corrispondere ad ogni sorgente un punto nel piano focale, e "concentra" il segnale, producendo un' immagine

$$C_B = B\, A_d\, \Delta E\, \Delta t$$

Background counts from a collimated telescope with detector area $A_d$, sensitive over the band $\Delta E$, in a time interval $\Delta t$

$$\sigma(C_B) = C_B^{1/2}$$

The counts obey the Poisson statistics

$$C_S = S_E\, A_d\, \Delta E\, \Delta t\, \eta_E$$

Source counts collected from a source with flux $S_E$ in the same conditions (QE=$\eta_E$)

$$C_{\text{meas}} = (C_S + C_B) - C_B$$

Measured counts (backg-subtracted)

$$\sigma^2(C_{\text{meas}}) = 2\sigma^2(C_B)$$

Background dominates fluctuations

$$S/N = n_\sigma = \frac{C_S}{\sqrt{2C_B}} = \frac{S_E\, A_d\, \Delta E\, \Delta t\, \eta_E}{\sqrt{2B\, A_d\, \Delta E\, \Delta t}}$$

$$S_{E,\text{min}} = \frac{n_\sigma}{\eta_E} \frac{\sqrt{2B}}{\sqrt{A_d\, \Delta t\, \Delta E}}$$

# X-Ray Mirrors

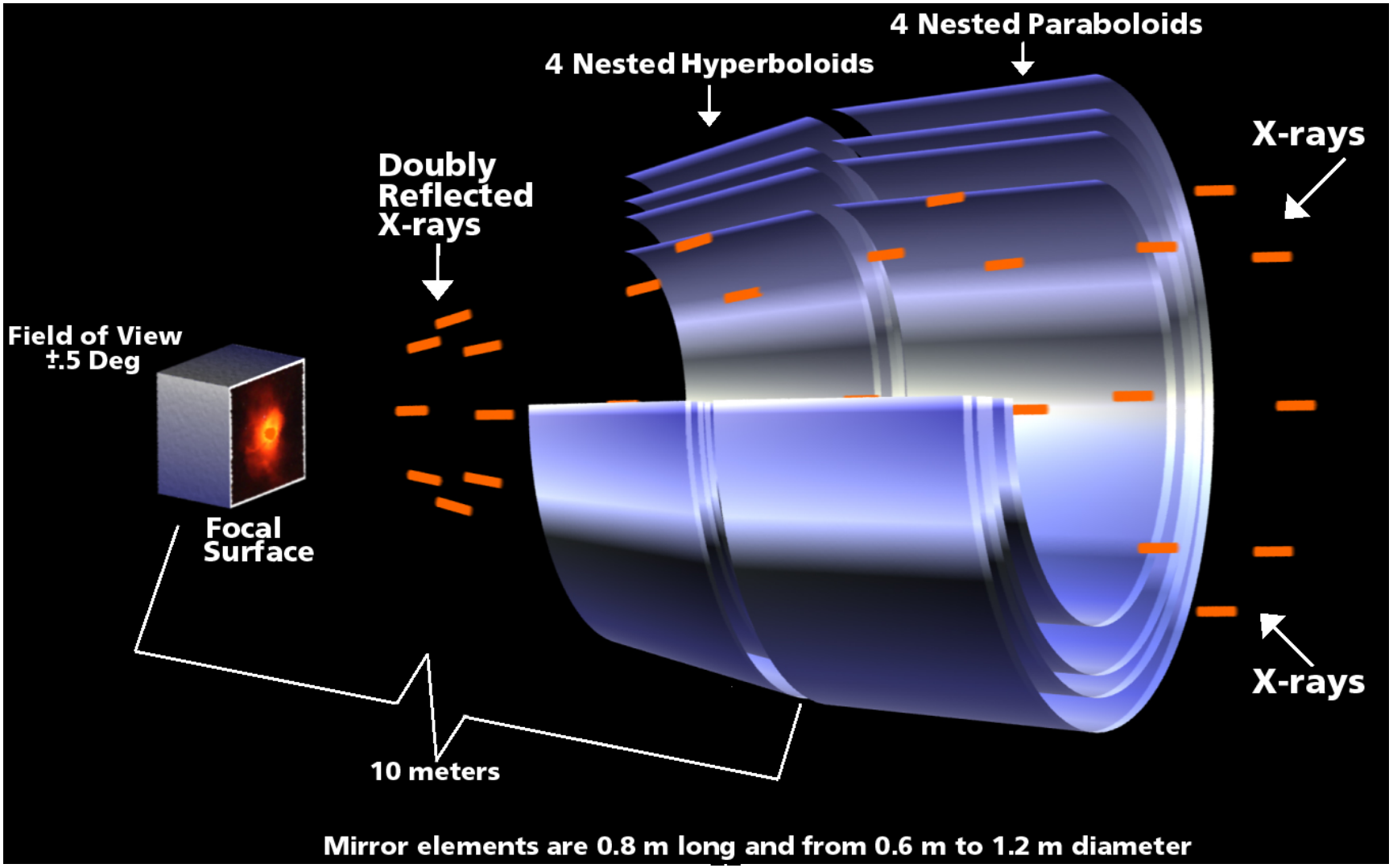

# *Why do we use X-ray optics*

- To achieve the best 2-dim angular resolution
    - To distringuish nearby sources or different regions of the same source
    - To perform morphological studies
- As a collector to “gather” weak fluxes (case of limited photon statistics)
- As a concentrator, so that the image photons may interact in a small region of the detector, thus limiting the influence of the background
- To serve with high spectral resolution dispersive spectrometers such as transmission or reflection gratings
- To simultaneously measure both the source(s) of interest and the contaminating background in other (source-free) regions of the detector

# X-ray optical constants

- X-rays are hard to refract or reflect: the refractive index of all materials in X-rays is very close to 1 and only slightly less than 1 ➔ X-rays are above the characteristic energy of bonded e- in atoms
- complex index of refraction of the reflector to describe the interaction X-rays /matter (see, for a review, Aschembach et al. 1985, Rep. Prog. Phys. 48, 579)

$$n=1-\delta+i\beta$$

where δ describes the phase change and β accounts for the absorption

δ and β depend on the wavelength

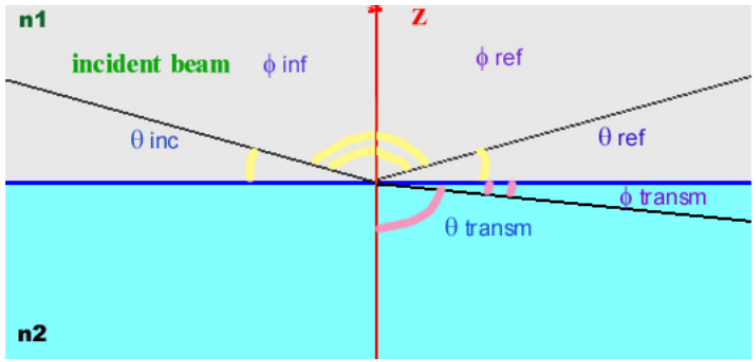


- the amplitute of reflection is described by the Fresnel's equations

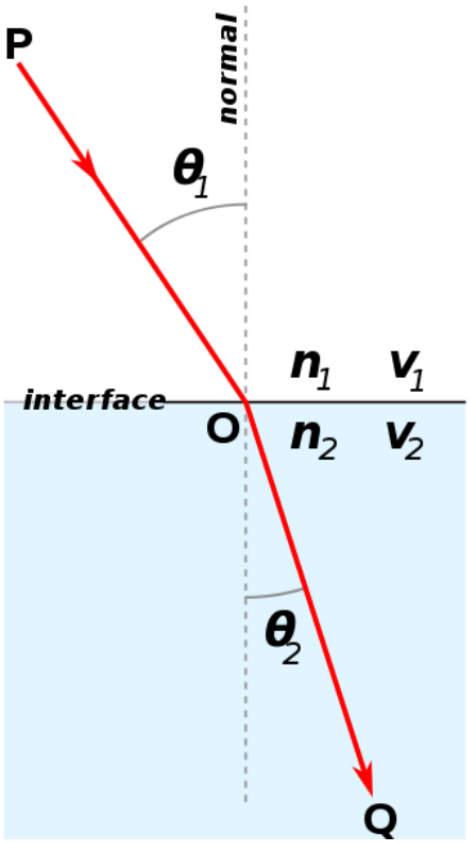


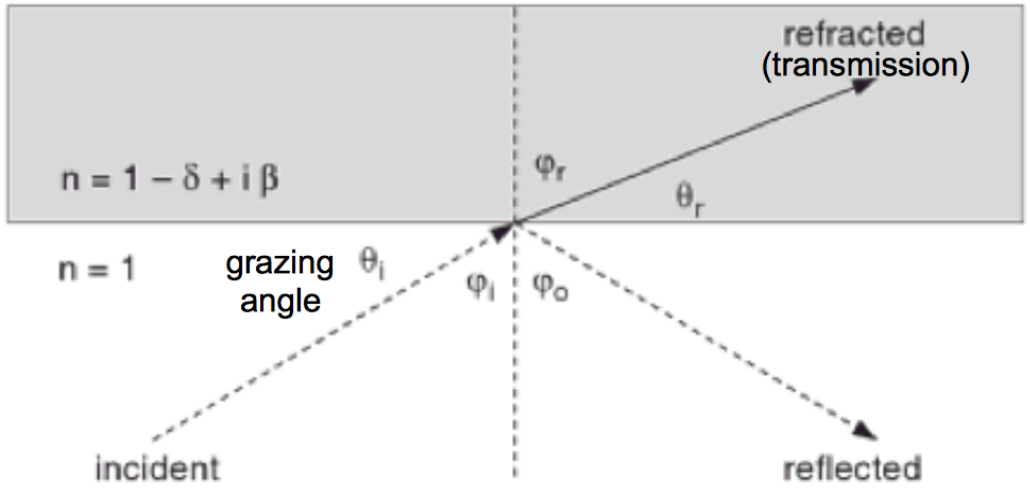


Snell's Law of Refraction:
relationship between the angles of incidence and refraction in a medium

$$n_1 \sin\theta_1 = n_2 \sin\theta_2$$

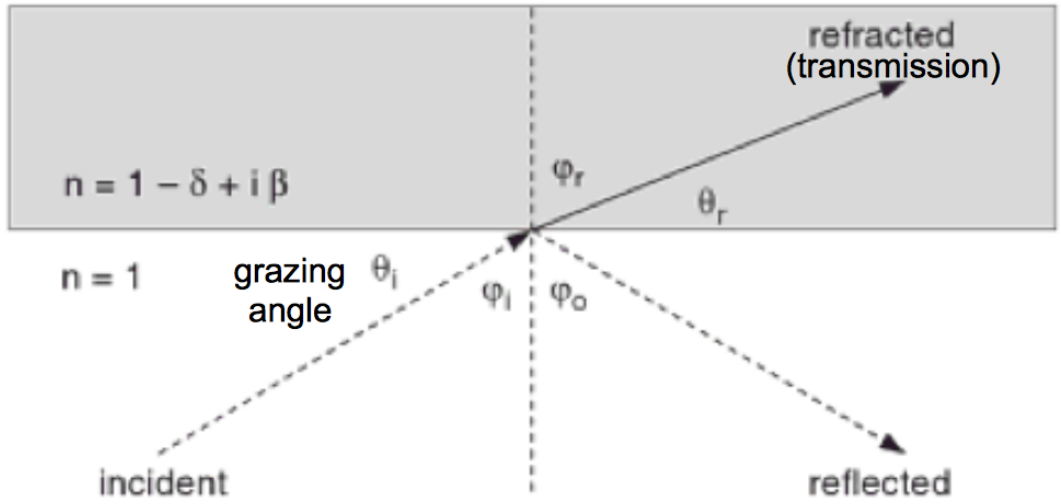


$$n_1 = 1,\ n_2 = (1-\delta) \rightarrow \sin\phi_i = (1-\delta)\sin\phi_r$$

$$\vartheta = (\pi/2) - \phi$$

$$\cos(90-\phi_i) = \cos\vartheta_i = (1-\delta)\cos(90-\phi_r) = (1-\delta)\cos\vartheta_r$$

$$\Rightarrow \cos\vartheta_i = \cos\vartheta_r(1-\delta)$$

Total reflection if no real solution for $\vartheta_r$

$\delta>0$, $\cos\theta_r \leq 1$ ➔ There is a **critical angle $\theta_c$** below which refraction is impossible and total external reflection occurs (grazing angle, $\theta_i=\theta_c$)

Extreme case for low θr values

$$1 = \cos\vartheta_r = \cos\vartheta_c/(1-\delta) \rightarrow \cos\vartheta_c = 1-\delta$$

# Total X-ray reflection at grazing incidence

- Real part of n slightly less than unity for matter at X-rays, =1 in vacuum (total external reflection); $\delta << 1$
- Snell's law ($n1 \cos\theta_1 = n2 \cos\theta_2$) to find a critical angle for total reflection
- (Total) external reflection in vacuum for angles < critical angle: $\cos\theta_{crit} = 1 - \delta$
- X-ray partially reflected also for $\theta > \theta_{crit}$; also, some absorption in the material
- $\cos(\theta_{crit}) = 1 - \theta_{crit}^2/2 = 1 - \delta \xrightarrow{\text{low angles}} \theta_{crit} = \sqrt{2\delta}$
- Far from fluorescent edges: $\delta \approx \frac{N_0 Z r_e \rho \lambda^2}{2\pi A}$

where $N_0$=Avogadro's number
Z=atomic number
$r_e$=electron radius
ρ=density
λ=wavelength of the incoming photon
A=atomic weight

Critical angle:

- Inversely dependent on energy
- Higher Z materials reflect higher energies, for a fixed grazing angle
- Higher Z materials have a larger critical angle at any energy

- For heavy elements, Z/A≈0.5, and if δ<<1:

$$\theta_{crit} \approx \sqrt{2\delta} \approx 5.6\lambda\sqrt{\rho}$$

where λ[Å] and ρ[g/cm³], and θ[arcmin]

$$\theta_{crit} \propto \sqrt{\rho} / E$$

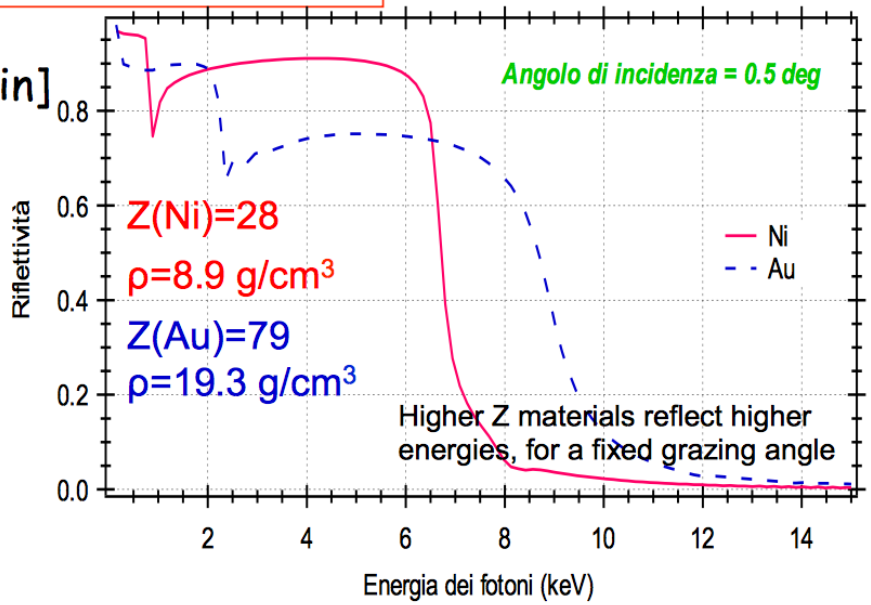


- Some reflectivity is lost due to scattering related to the presence of micro-roughness at the surface

- Use of heavy materials (but attention at the absorption edges…)

# X-ray mirrors with parabolic profile

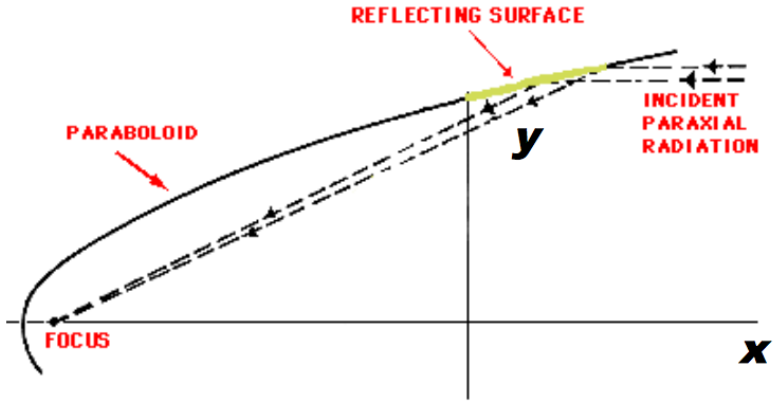


- perfect on-axis focusing
- off-axis images strongly affected by coma

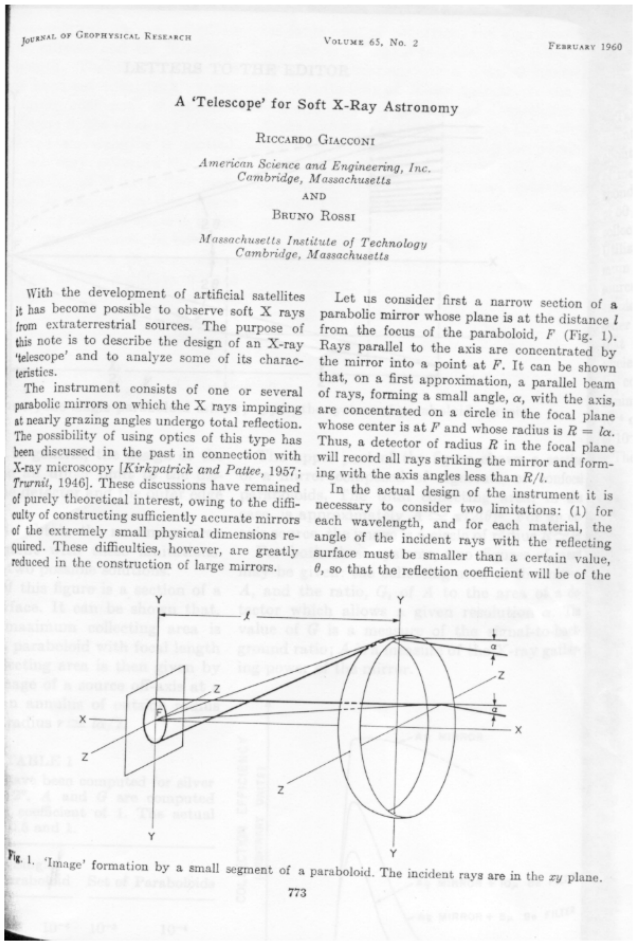

JOURNAL OF GEOPHYSICAL RESEARCH VOLUME 65, No. 2 FEBRUARY 1960

A 'Telescope' for Soft X-Ray Astronomy

RICCARDO GIACCONI

*American Science and Engineering, Inc.*
*Cambridge, Massachusetts*

AND

BRUNO ROSSI

*Massachusetts Institute of Technology*
*Cambridge, Massachusetts*

With the development of artificial satellites it has become possible to observe soft X rays from extraterrestrial sources. The purpose of this note is to describe the design of an X-ray 'telescope' and to analyze some of its characteristics.

The instrument consists of one or several parabolic mirrors on which the X rays impinging at nearly grazing angles undergo total reflection. The possibility of using optics of this type has been discussed in the past in connection with X-ray microscopy [*Kirkpatrick and Pattee*, 1957; *Trurnit*, 1946]. These discussions have remained of purely theoretical interest, owing to the difficulty of constructing sufficiently accurate mirrors of the extremely small physical dimensions required. These difficulties, however, are greatly reduced in the construction of large mirrors.

Let us consider first a narrow section of a parabolic mirror whose plane is at the distance $l$ from the focus of the paraboloid, $F$ (Fig. 1). Rays parallel to the axis are concentrated by the mirror into a point at $F$. It can be shown that, on a first approximation, a parallel beam of rays, forming a small angle, $\alpha$, with the axis, are concentrated on a circle in the focal plane whose center is at $F$ and whose radius is $R = l\alpha$. Thus, a detector of radius $R$ in the focal plane will record all rays striking the mirror and forming with the axis angles less than $R/l$.

In the actual design of the instrument it is necessary to consider two limitations: (1) for each wavelength, and for each material, the angle of the incident rays with the reflecting surface must be smaller than a certain value, $\theta$, so that the reflection coefficient will be of the

Fig. 1. 'Image' formation by a small segment of a paraboloid. The incident rays are in the $xy$ plane.

773

Wolter, 1952

# Wolter's solution to the X-ray imaging

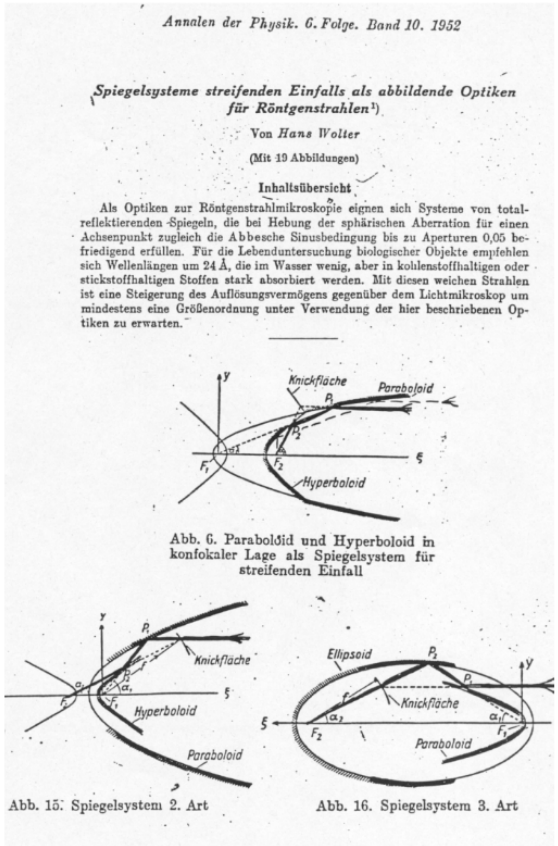

*Annalen der Physik. 6. Folge. Band 10. 1952*

***Spiegelsysteme streifenden Einfalls als abbildende Optiken für Röntgenstrahlen***[1])

Von *Hans Wolter*

(Mit 19 Abbildungen)

**Inhaltsübersicht**

Als Optiken zur Röntgenstrahlmikroskopie eignen sich Systeme von totalreflektierenden Spiegeln, die bei Hebung der sphärischen Aberration für einen Achsenpunkt zugleich die Abbesche Sinusbedingung bis zu Aperturen 0,05 befriedigend erfüllen. Für die Lebenduntersuchung biologischer Objekte empfehlen sich Wellenlängen um 24 Å, die im Wasser wenig, aber in kohlenstoffhaltigen oder stickstoffhaltigen Stoffen stark absorbiert werden. Mit diesen weichen Strahlen ist eine Steigerung des Auflösungsvermögens gegenüber dem Lichtmikroskop um mindestens eine Größenordnung unter Verwendung der hier beschriebenen Optiken zu erwarten.



Abb. 6. Paraboloid und Hyperboloid in konfokaler Lage als Spiegelsystem für streifenden Einfall



Abb. 15. Spiegelsystem 2. Art



Abb. 16. Spiegelsystem 3. Art

H. Wolter, Ann. Der Phys., NY10, 94 (1952)

Fine for X-ray astronomy **a**

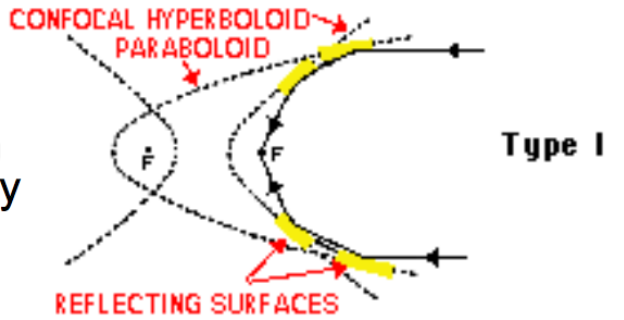


Applied in solar X-ray telescopes **b**

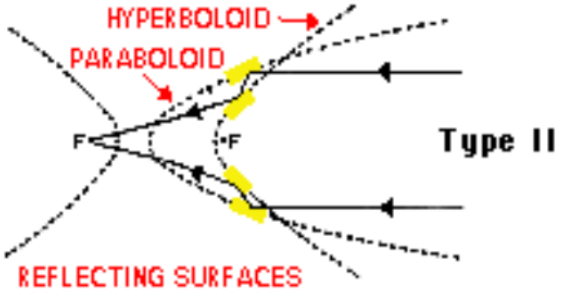


Not adopted **c**

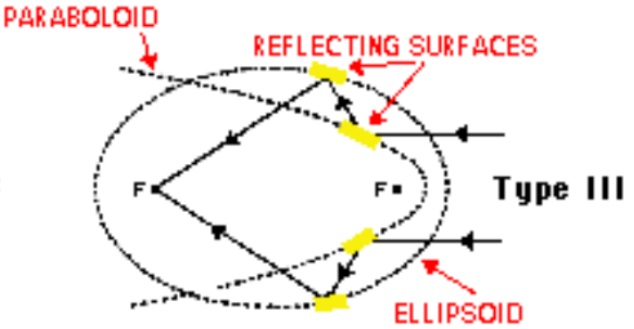

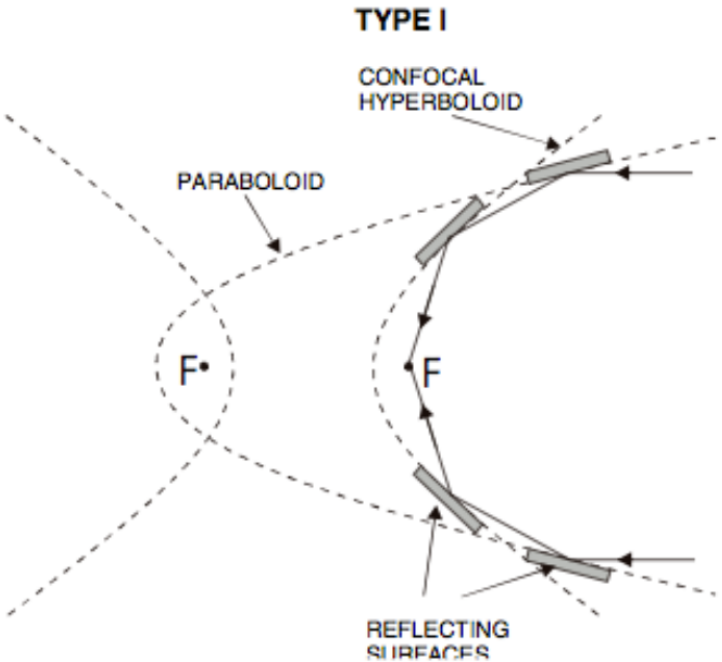


**Wolter-I optics**

Paraboloid ➔ Hyperboloid

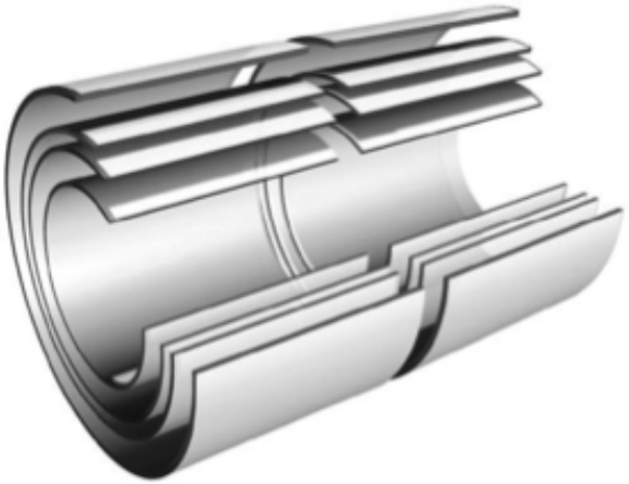

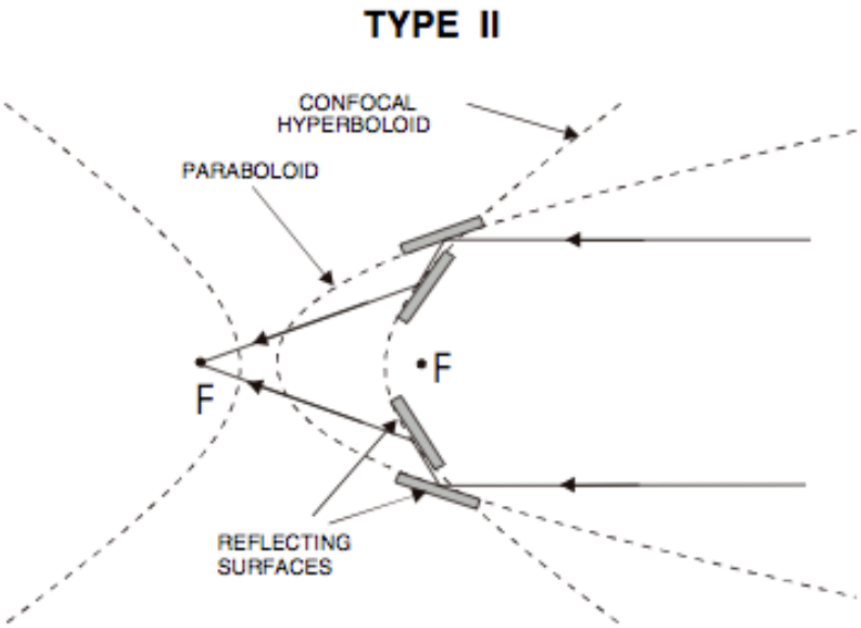


**Wolter-II optics**

Paraboloid ➔ Hyperboloid (ext. surface)

# X-Ray Mirrors

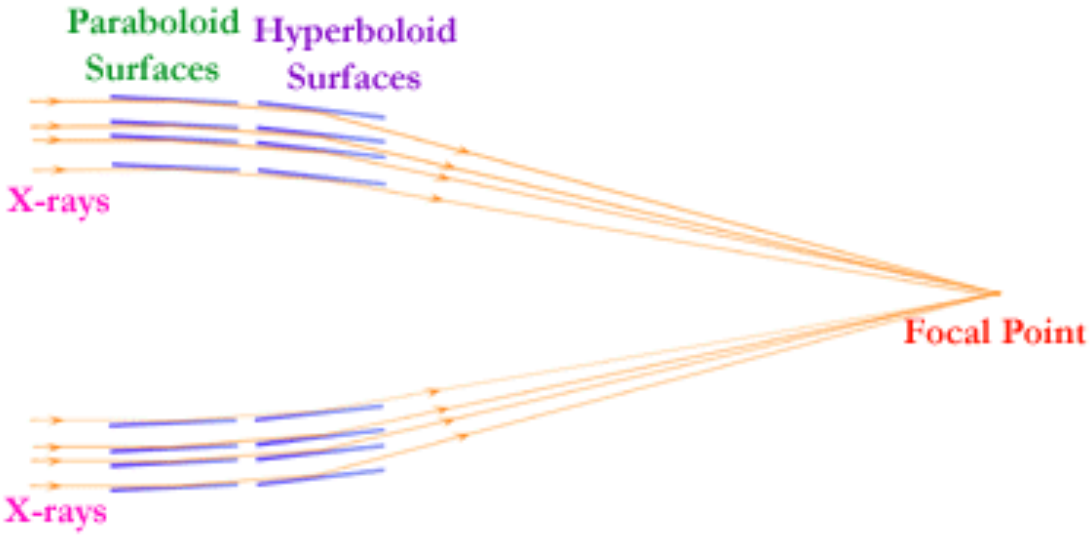


$$\cos\phi = 1 - \delta$$

$$\delta = 2.70 \times 10^{-6} \frac{Z_e}{A} \rho\lambda^2$$

Cf Aschembach et al. 1985

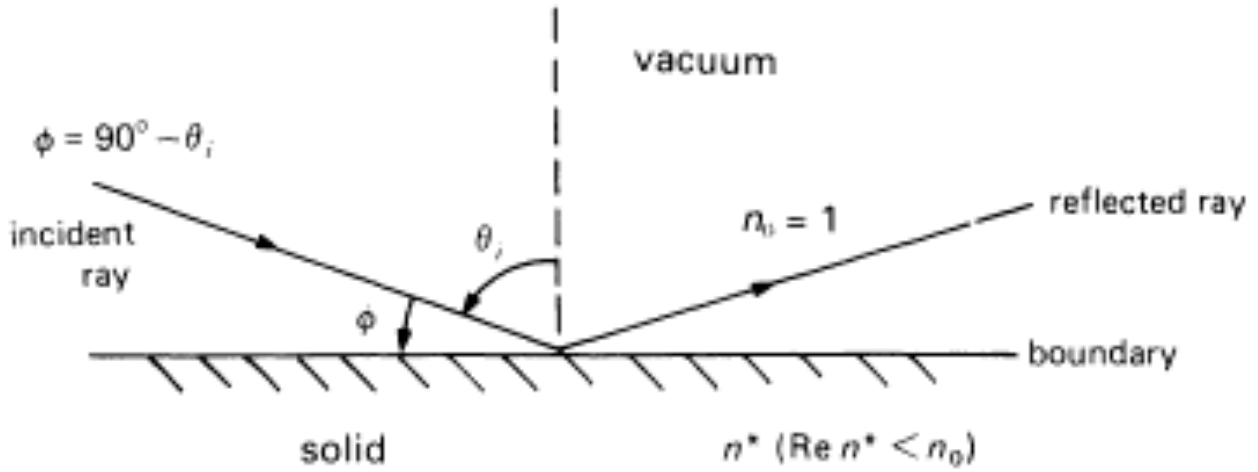

## $A_{geom}$ x Reflectivity

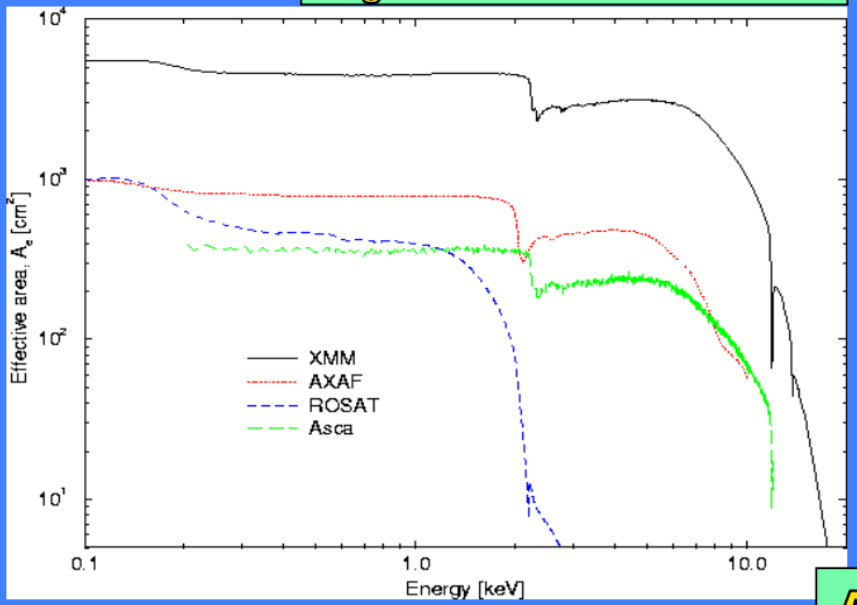


x

## QE

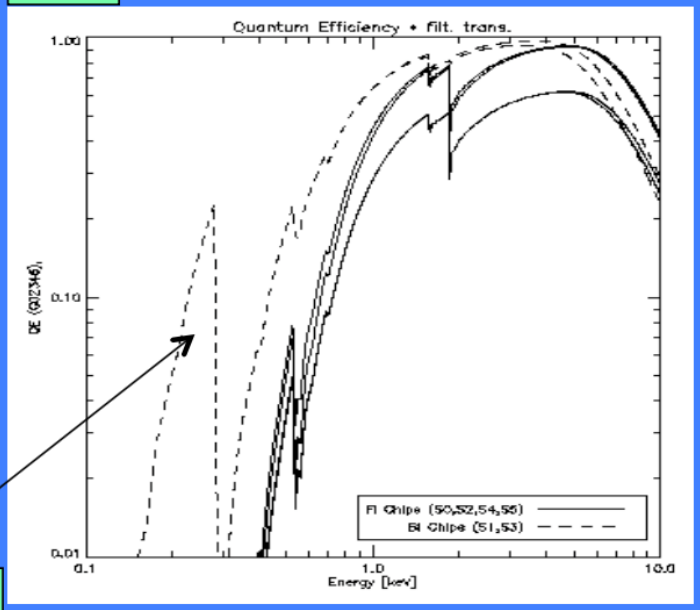


## $A_{effective}$

=

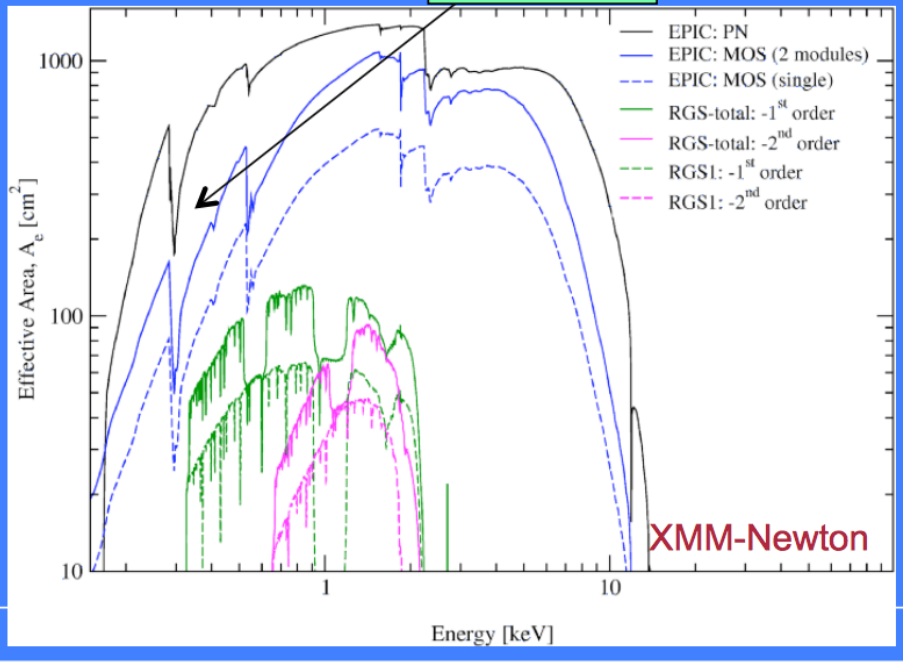


## CCD

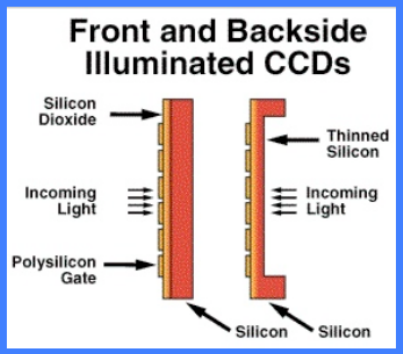

# Focalizzazione vs collimazione

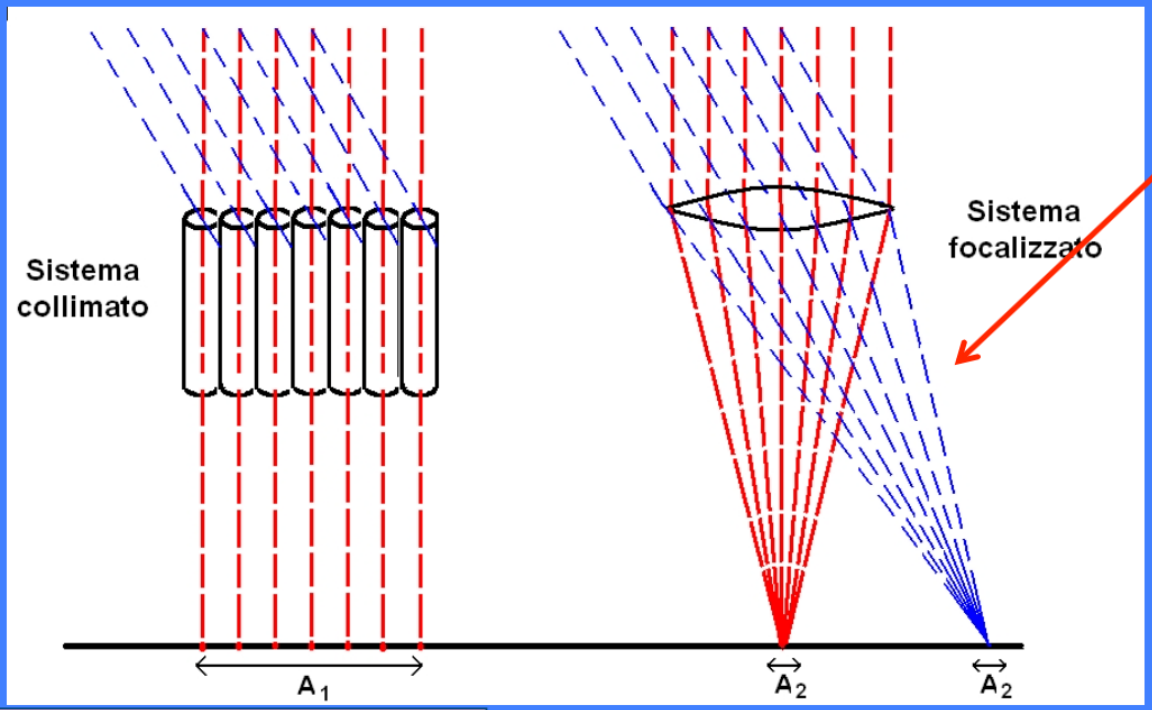


Proper imaging of X-rays below 20-40 keV

$$F_{\min} \approx n_\sigma \frac{\sqrt{2B}}{\sqrt{A_{\det} T_{\text{int}} \Delta E}}$$

$A_d$= PSF projected on the focal plane

$$F_{\min} \approx n_\sigma \frac{\sqrt{B A_d}}{A_{eff} \sqrt{T_{\text{int}} \Delta E}}$$

**Sistema collimato**: limita la regione di cielo da cui puo' provenire un segnale, (quindi limita il background), non incrementandone la "densita"

**Sistema focalizzato**: fa corrispondere ad ogni sorgente un punto nel piano focale, e "concentra" il segnale, producendo un' immagine

$$C_S = S_E \, A_e \, \Delta E \, \Delta t \, \eta_E$$

Detected signal

$$C_B = B \, \varepsilon \, A_d \, \Delta E \, \Delta t$$

Background signal (ε: region of the detector where B counts are focused)

$$S/N = n_\sigma = \frac{C_S}{\sqrt{C_S + 2C_B}} \approx \frac{S_E \, A_e \, \Delta E \, \Delta t \, \eta_E}{\sqrt{2B \, \varepsilon \, A_d \, \Delta E \, \Delta t}}$$

$$S_{E,\min} = \frac{n_\sigma}{\eta_E} \, \frac{1}{A_e} \sqrt{\frac{2B \, \varepsilon \, A_d}{\Delta t \, \Delta E}}$$

Weak sources

# Old slide but *Chandra* and XMM-*Newton* still working

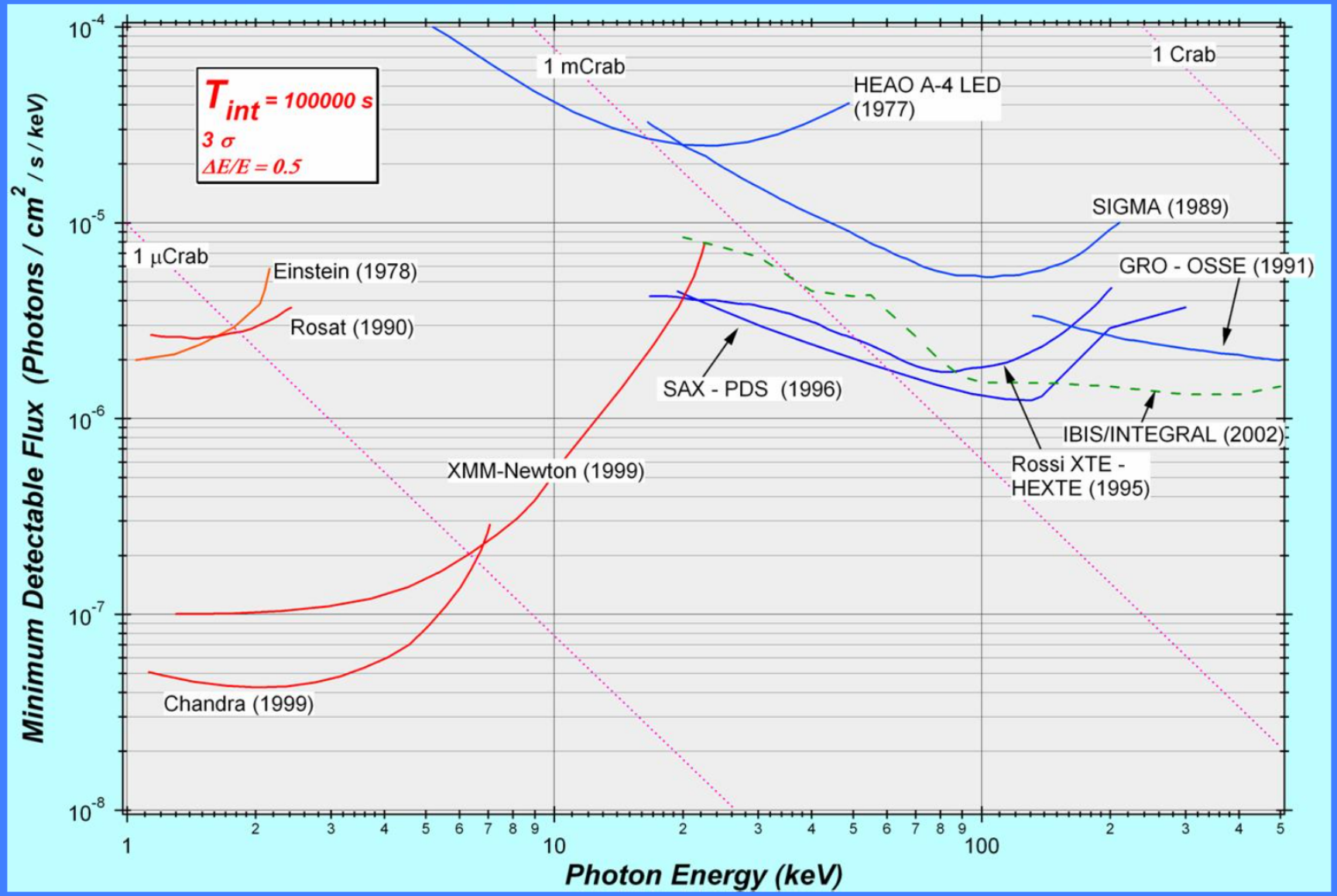

# Single photon calorimeter

**Individual X-ray photons are absorbed by a crystal which is maintained at a T very close to absolute zero (<0.1 K).**
**➔ 2-3 year lifetime**

**We measure the increase of T which is proportional to the energy of the X-ray photon**

**Energy resolution ~ 3 eV**

**High efficiency**

**The best spectral resolution of any non-dispersive (grating) spectrometer**

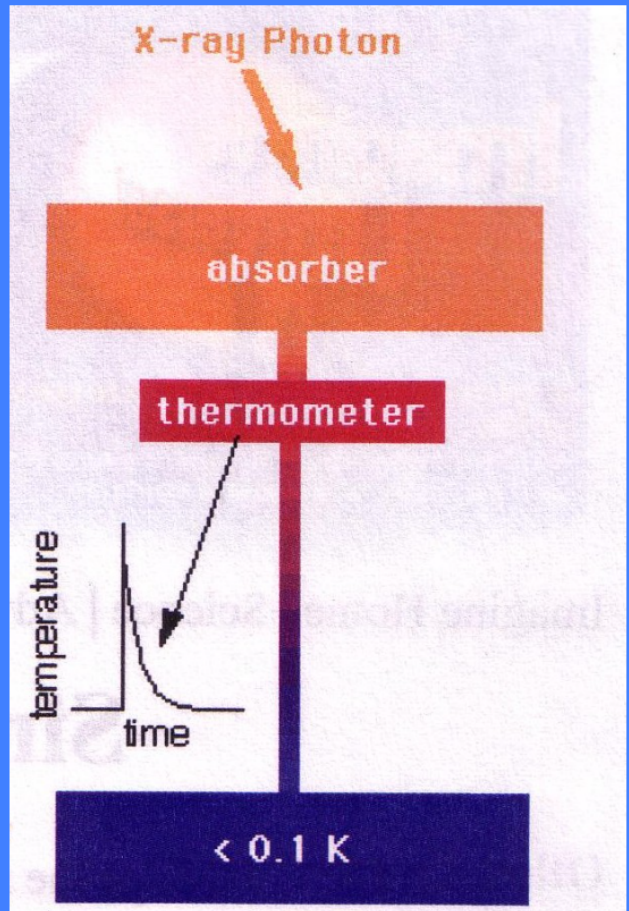


Diagram showing the essential elements of a calorimeter. Inset shows temperature response to an X-ray hit.

## Onboard *Suzaku* – calibration source ($^{55}$Fe)

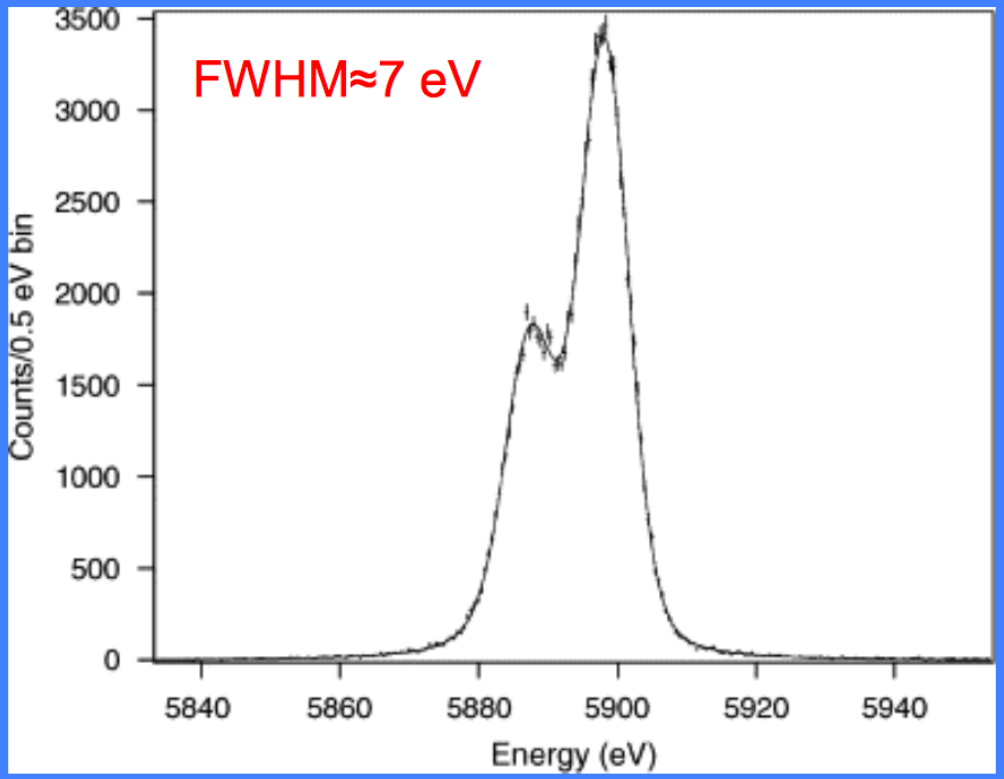


Expected spectral resolutions ≤2-3 eV in next-generation X-ray calorimeters (e.g., *Athena*)

Onboard of the Japanese mission ASTRO-H/*Hitomi* (

Last year ☹

# X-ray spectroscopy

## Telescopes and instruments

### Dispersing elements – Bragg Crystal spectroscopy/1

(more details on dispersive spectrometers: Giacconi & Gursky, p. 81-90)

**The reflection of X-rays from a crystal lattice follows the Bragg's law, and therefore the name Bragg spectrometer is usually given to the device with this kind of reflection grating.**

**Here the macroscopic shaping (grooves) of a metallic plate, which is used in longer wavelengths, is replaced by a material with regular lattice structure of atoms (crystal material). The reflection takes place by the same principle as from a macroscopic lattice, leading to a wavelength-dispersed output from a white light input.**

**The lattice of the crystal forms a 3-dimensional diffraction array which reflects X-rays of wavelength λ within a narrow range of wavelength satisfying the Bragg condition**

$$n\lambda = 2d\sin\theta \quad , n = 1,2,3,\ldots \text{ (order of diffraction)}$$

**where *d* is the crystal lattice spacing.**
**In practice, order n=1 is used.**

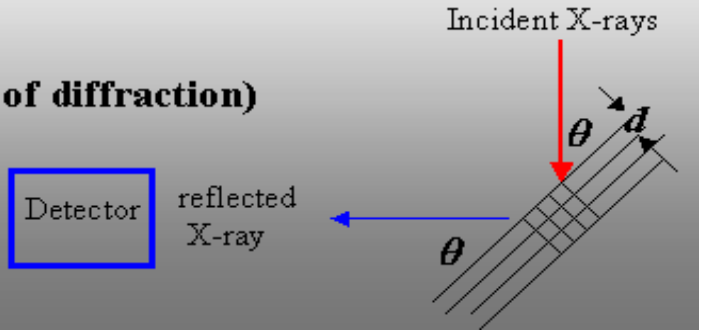

# X-ray spectroscopy

## Dispersing elements – Diffraction gratings/1

**Ordinary diffraction gratings can also be used from from long wavelengths up to soft X-rays (< 1 keV, in practice).**

**The grating equation is**

$$n\lambda = (1/N)\ (\sin\theta - \sin\theta_o),\ n = 1,2,3,\ldots \text{ (order of diffraction)}$$

**where N is the grating constant (lines/cm), $\theta$ is the diffraction angle and $\theta_o$ is the angle of incidence. For X-rays this is usually rearranged in form valid for small angles**

$$n\lambda N = \theta - \theta_o$$

**There are two geometries usually applied in X-ray optics,**

**1. Conventional Johann mount geometry**

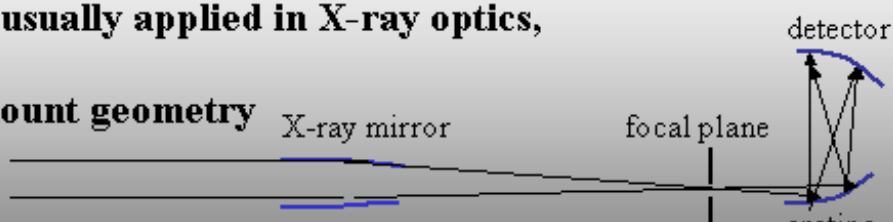


**2. Curved grating producing a line image**

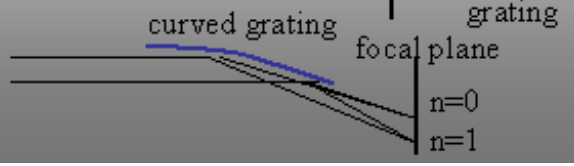

# X-ray polarimetry

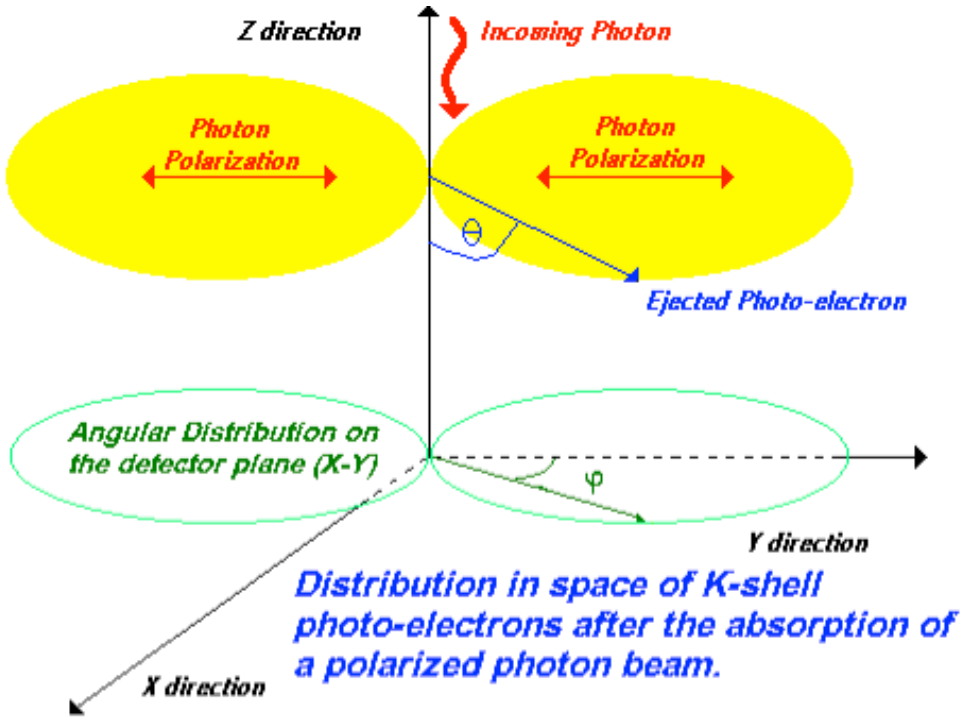


Costa et al. 2001

# X-ray polarimetry

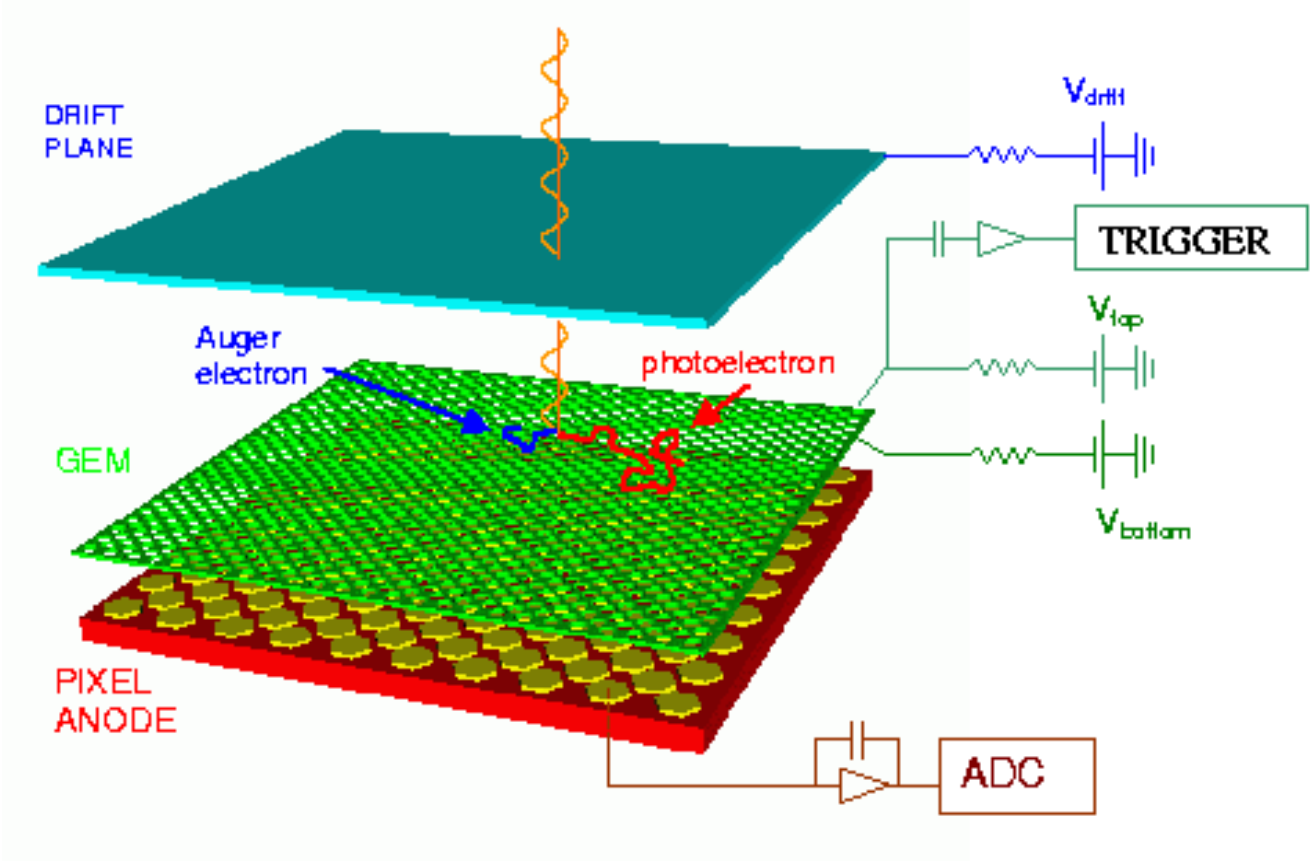

# X-ray imaging

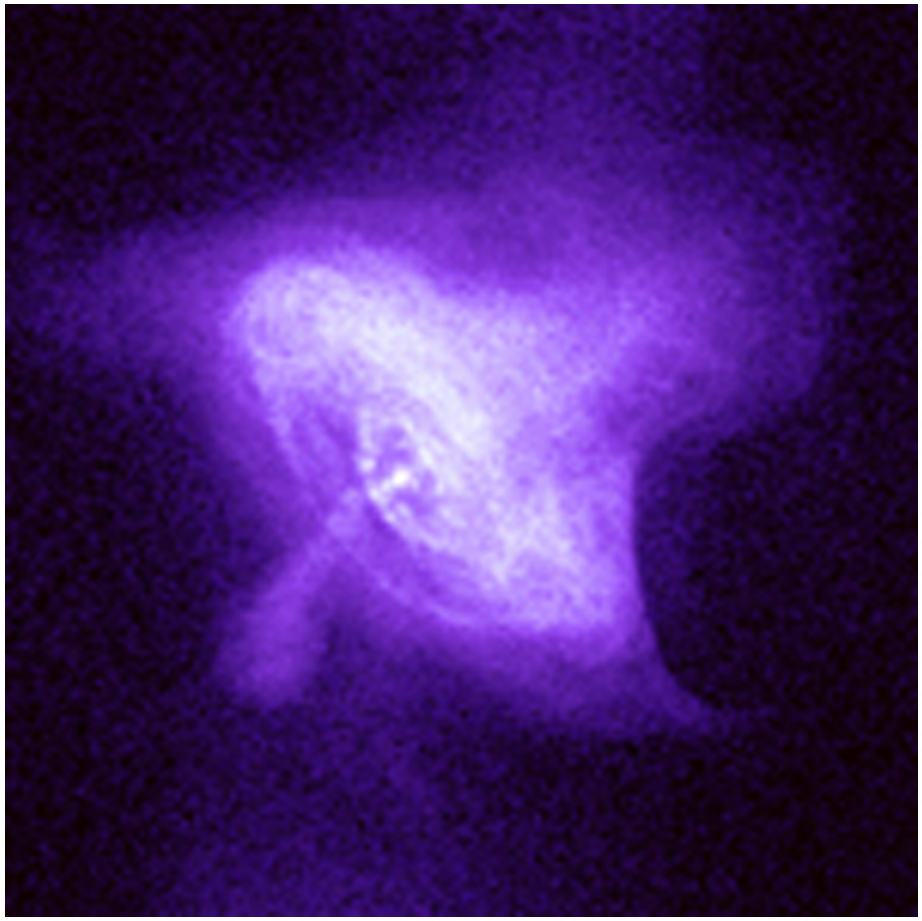

Crab nebula, 2.5”, 0.3 – 3 keV

# La risoluzione angolare in astronomia X: da *ROSAT* a *Chandra*

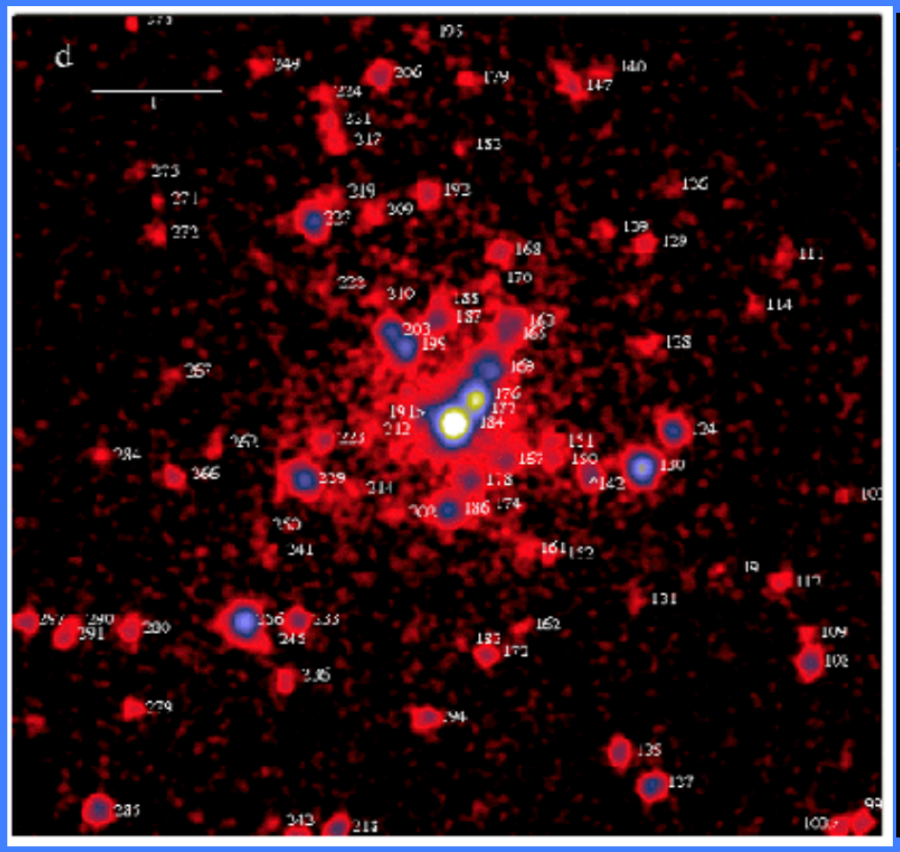

Osservazione di Orion
con ROSAT HRI (47 ks)

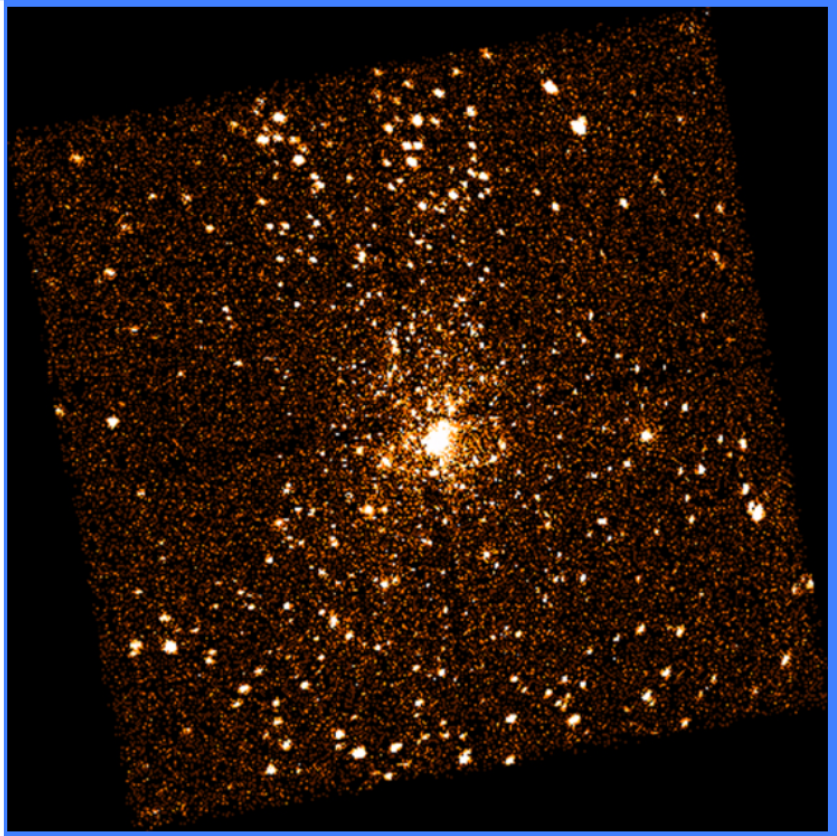

Osservazione di Orion
con Chandra ACIS (13.7 ks)

# X-ray spectroscopy

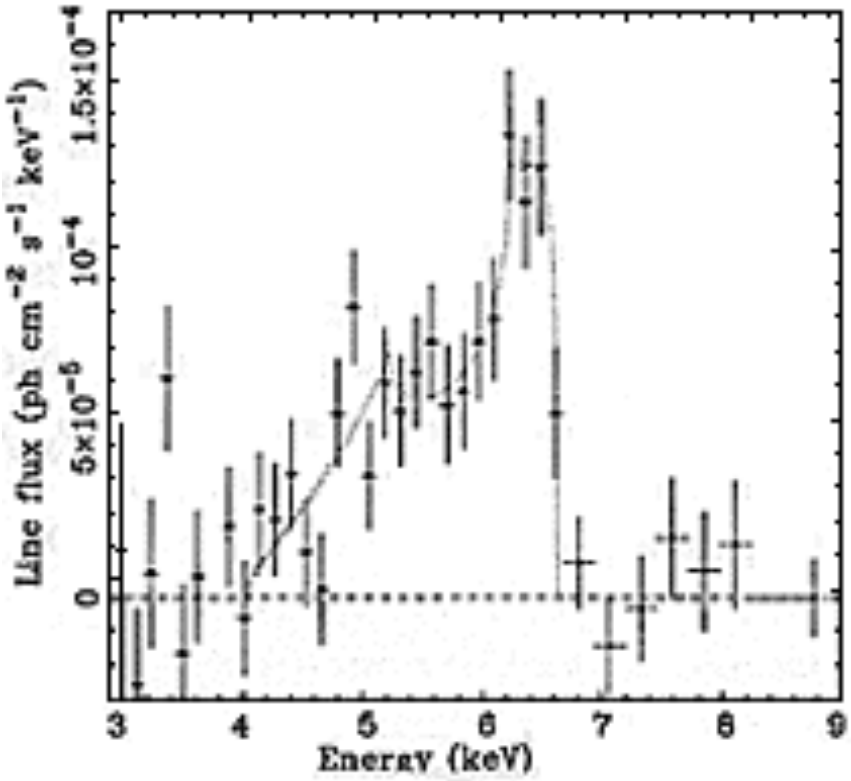


The Fe line profile of K-alpha in the X-ray emission from the active nucleus of the galaxy MCG 6-30-15 in the constellation Centaurs is powered by matter accreting into a black hole.

# ROSAT http://www.mpe.mpg.de/xray/wave/rosat/

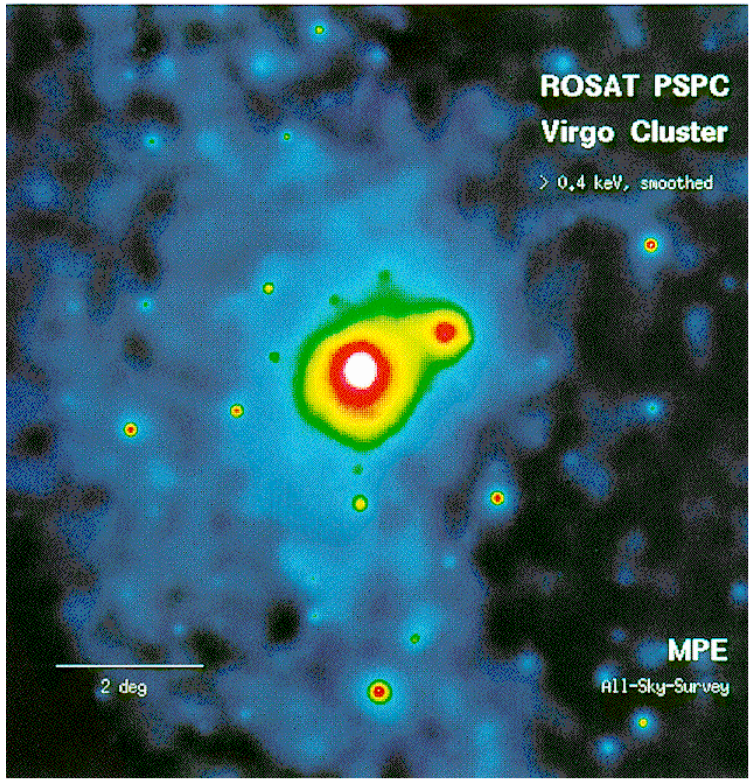


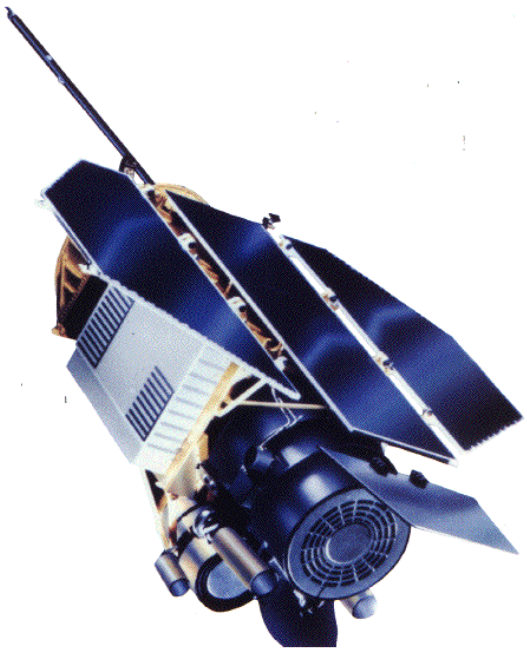

The scientific payload consists two coalligned scientific experiments, the The X-Ray Telescope which is used in conjunction with one of the focal plane instruments:

- The Position Sensitive Proportional Counter
- The High Resolution Imager

and the The Wide Field Camera which has its own mirror system and star sensor.
ROSAT provides a ~ 2 degree diameter field of view with the PSPC in the focal plane, and ~ 40 arcmin diameter field of view with the HRI in the focal plane. The ROSAT mission began with a six-month, all-sky PSPC survey,
after which the satellite began a series of pointed observations that continued for the duration of the project.

# ROSAT results

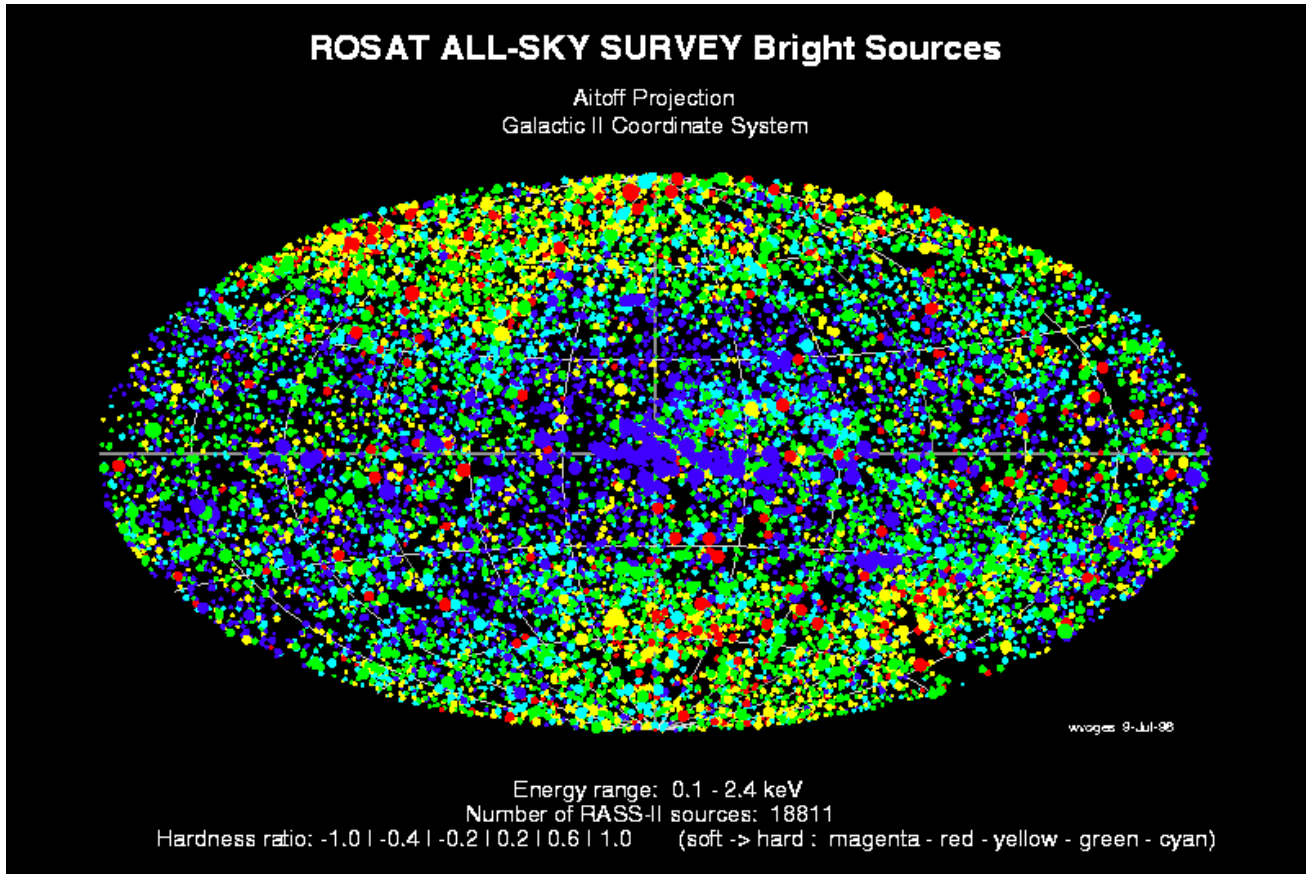


The ROSAT All-Sky Survey Bright Source Catalogue (RASS-BSC, revision 1RXS) is derived from the all-sky survey performed during the first half year of the ROSAT mission in 1990/91. 18,811 sources are catalogued, with a limiting ROSAT PSPC countrate of 0.05 cts/s in the 0.1-2.4 keV energy band. [47]

# RXTE http://heasarc.gsfc.nasa.gov/docs/xte/xtegof.html

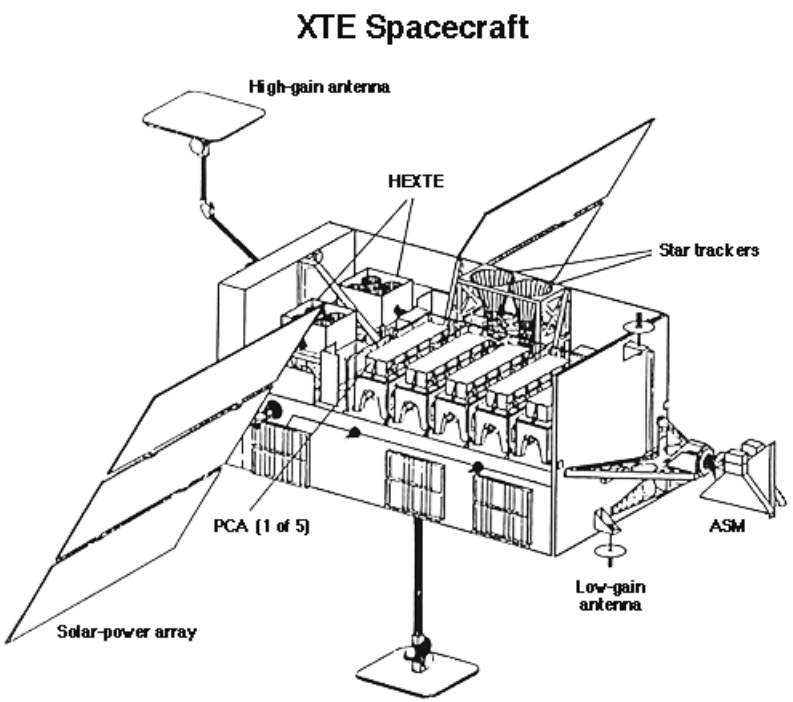


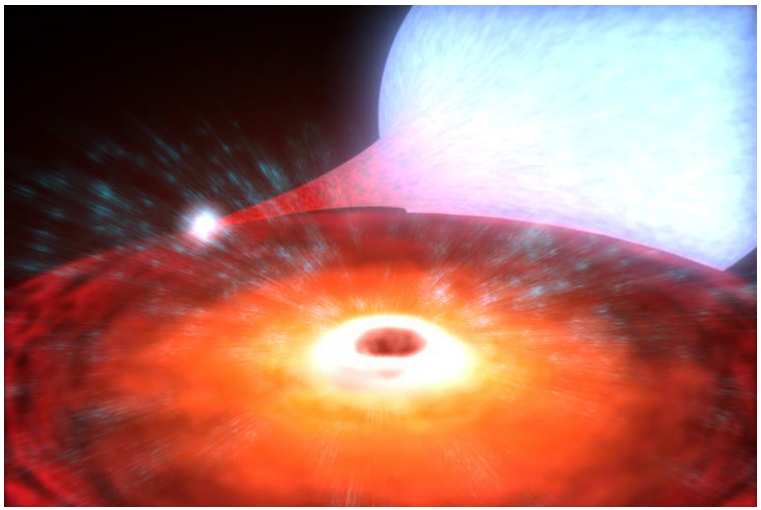

The lowest-mass known black hole belongs to a binary system named XTE J1650-500. The black hole has about 3.8 times the mass of our sun, and is orbited by a companion star

The Rossi X-ray Timing Explorer (RXTE) was launched on December 30, 1995.
RXTE features unprecedented time resolution in combination with moderate spectral resolution to explore the variability of X-ray sources. Time scales from microseconds to months are covered in an instantaneous spectral range from 2 to 250 keV.
Originally designed for a required lifetime of two years with a goal of five, it operated up to 2012

# BeppoSAX

http://www.asdc.asi.it/bepposax

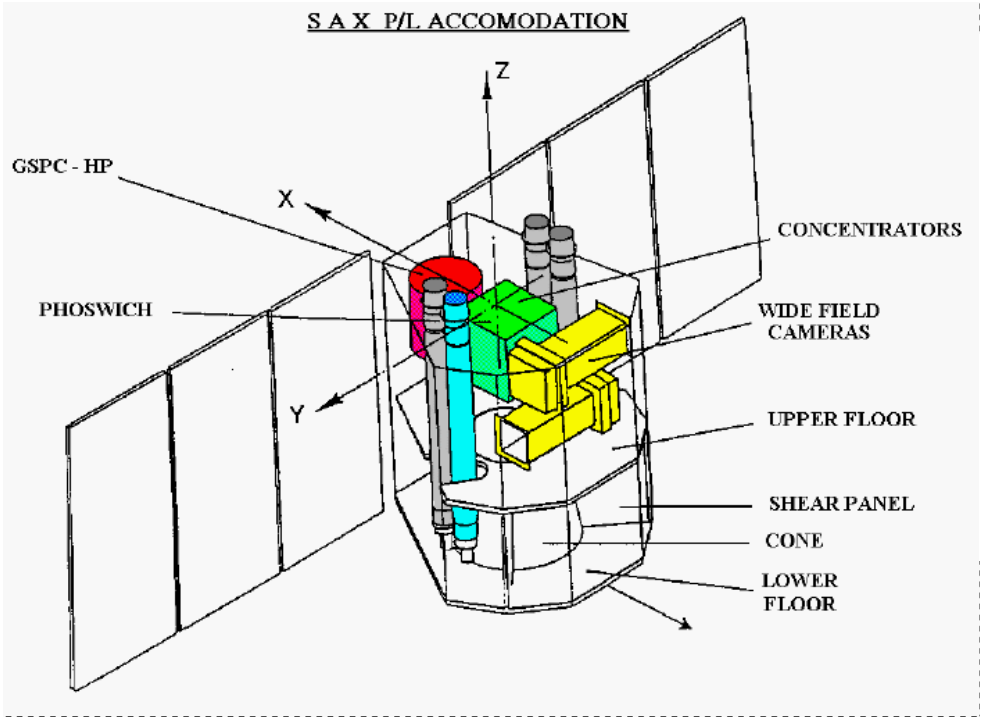


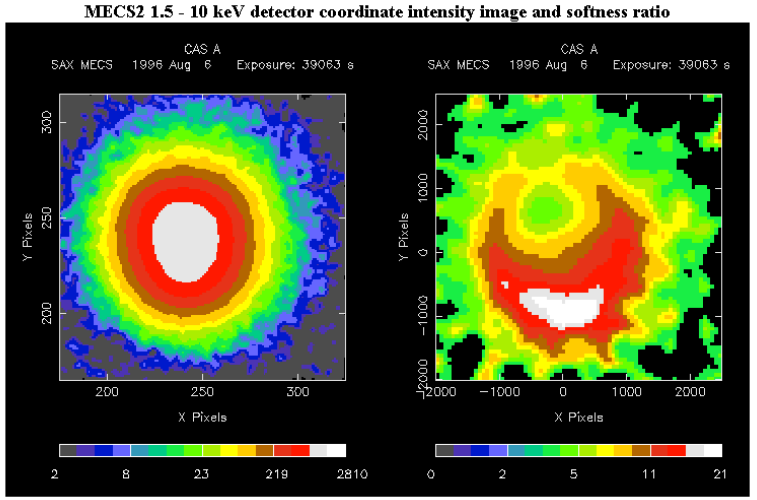


- **Energy Range 0.1 to 200 keV**
- **Imaging capabilities (1') in the range of 0.1-10 keV.**
- **High energy (3-300 keV)**
- **Narrow fields and point in the same direction (Narrow Field Instruments, NFI).**
- **Monitoring large regions of the sky with a resolution of 5' in the range 2-30 keV**
  **- two coded mask proportional counters pointing in diametrically opposed directions perpendicular to the NFI**
- **Anticoincidence scintillator shields of the PDS will be used as a gamma-ray burst monitor in the range 60-600 keV.**

# BeppoSAX results

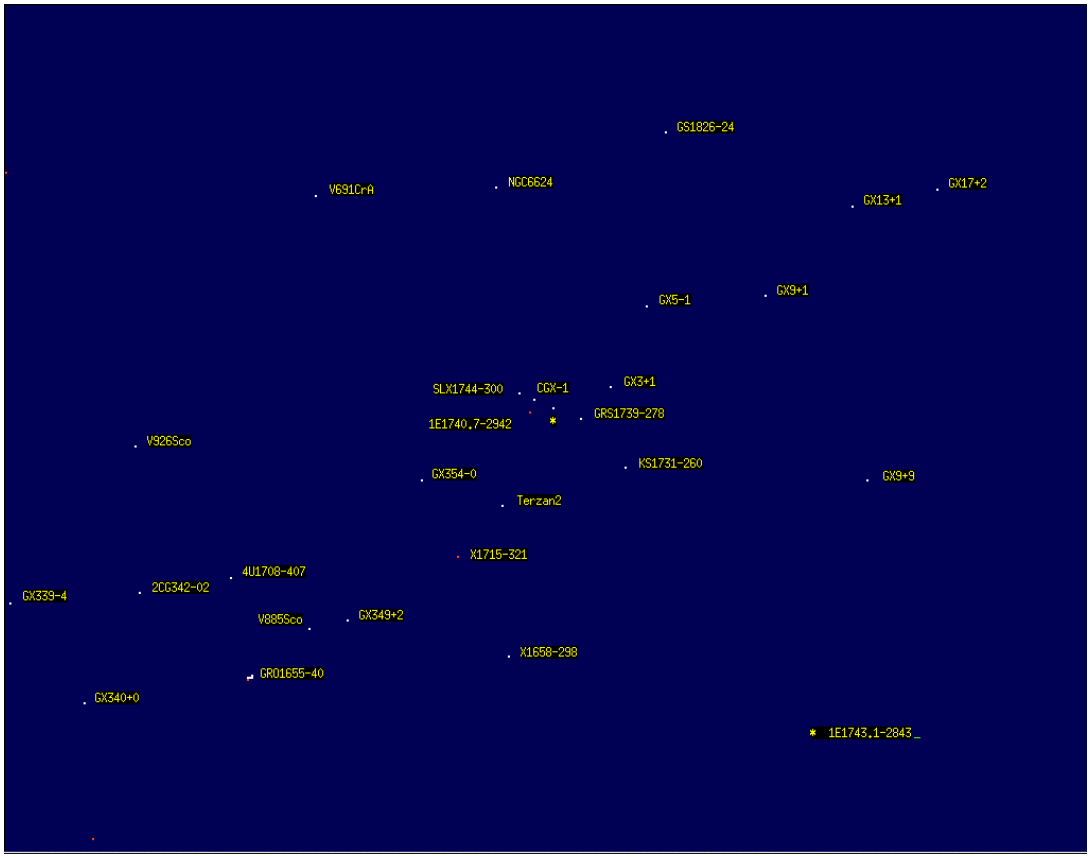


The Galactic Centre has been observed with the Beppo SAX Wide Field Camera 1 (WFC1) in August 1996.
Here an image is shown of the 40 degrees by 40. The observation period was from 22-8-1996 07.54 UT through to 23-8-1996 11.38 UT, while the effective exposure totalled about 51 kiloseconds. The number of accepted events was 1.7955 x 10^7 in the energy range of 5.4 - 11.3 keV. The legenda for the galactic centre source indicated with a yellow star (1E1743.1-2843), is given at lower right in the image.



To our knowledge this is the largest field ever imaged in X-rays in a single pointing.

# Chandra X-ray Telescope

http://chandra.harvard.edu/

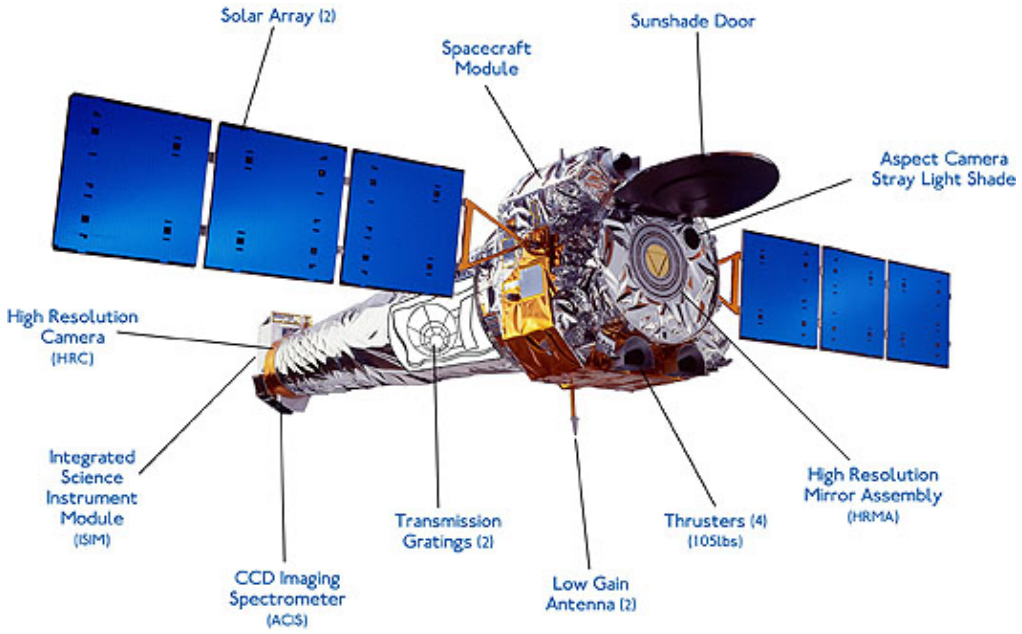


High resolution mirror
two imaging detectors
two sets of transmission gratings.
Spatial resolution: 0.5”
Good sensitivity from 0.1 to 10 keV
High spectral resolution $E/\Delta E = 1000$

# XMM-Newton

http://sci.esa.int/xmm-newton/

**XMM** carries the X-ray telescopes with the largest effective area.
58 thin nested mirror shells in each X-ray telescope.
Moderate and high spectral resolution.
Simultaneous optical/UV observations
Spatial resolution: 6”
Energy Range 0.2 to 12 keV
High Spectral resolution at LowE $E/\Delta E = 300$
Wide FoV

# Comparison

**A Comparison with other X-Ray Satellites**

The following table compares XMM with selected previous X-ray satellites:

| | ROSAT | ASCA | Chandra | XMM |
|---|---|---|---|---|
| Mirror effective area @ 1.0 keV (cm2) | 400 | 350 | 800 | 4650 |
| Imaging effective area @ 1.0 keV (cm2) | 200 | ... | 400 | 2400 |
| Spectroscopy effective area @ 1.0 keV (cm2) | - | - | 50 | 185 (orders 1+2) |
| Spectroscopic resolving power at 0.5 keV (E/dE) | (1) | 9 | 400-1000 | 500 |
| Mirror Resolution (arcsec) | 3.5 | 73 | 0.2 | 6 |
| CCD energy range (keV) | 0.1-2.4 | 0.5-10 | 0.1-10 | 0.1-15 |
| Orbit target visibility (hrs) | 1.3 | 0.9 | 50 | 40 |

# Chandra results

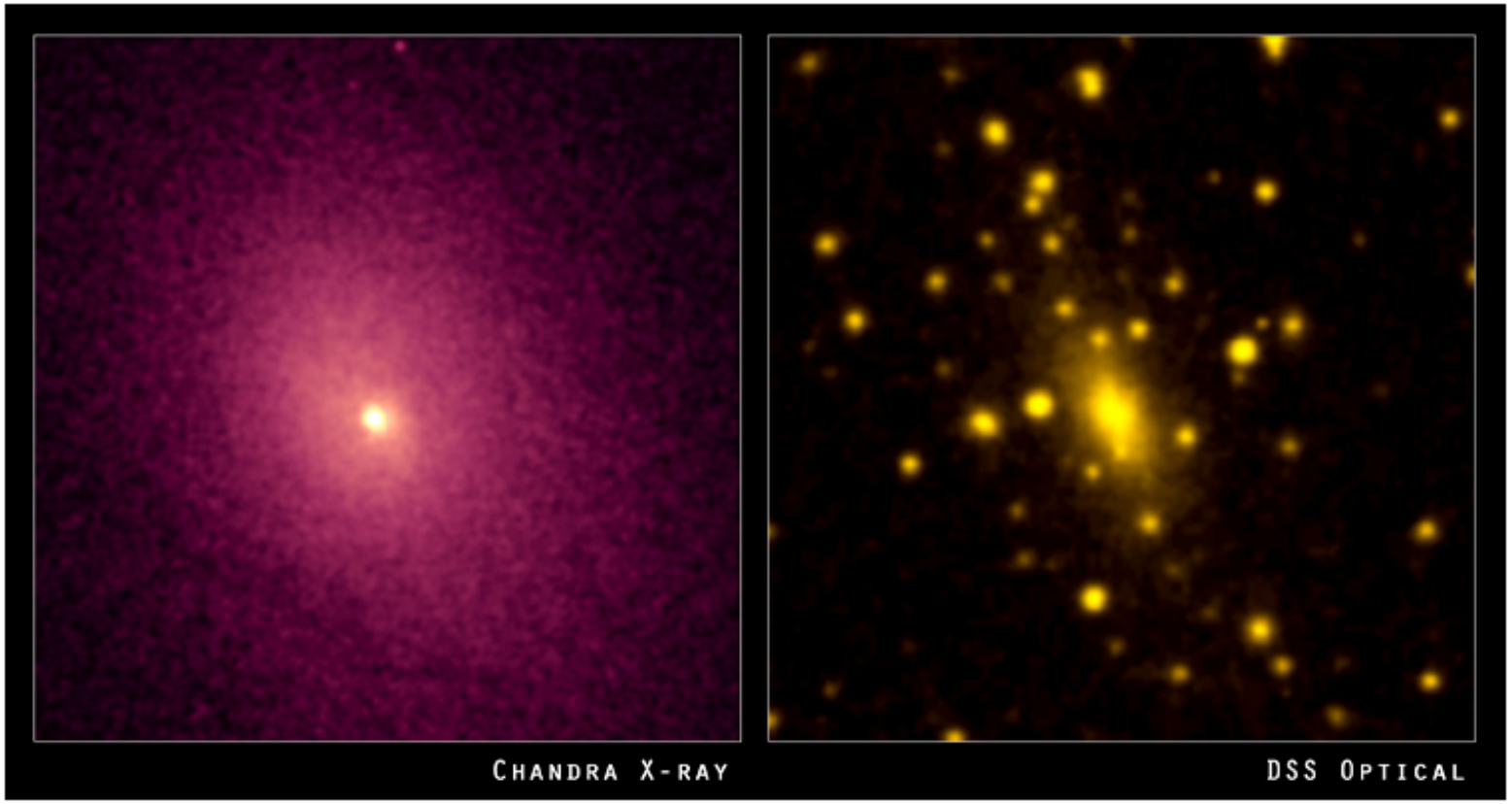


The galaxy cluster Abell 2029 is composed of thousands of galaxies (optical image) enveloped in a gigantic cloud of hot gas (X-ray image)

# Chandra results

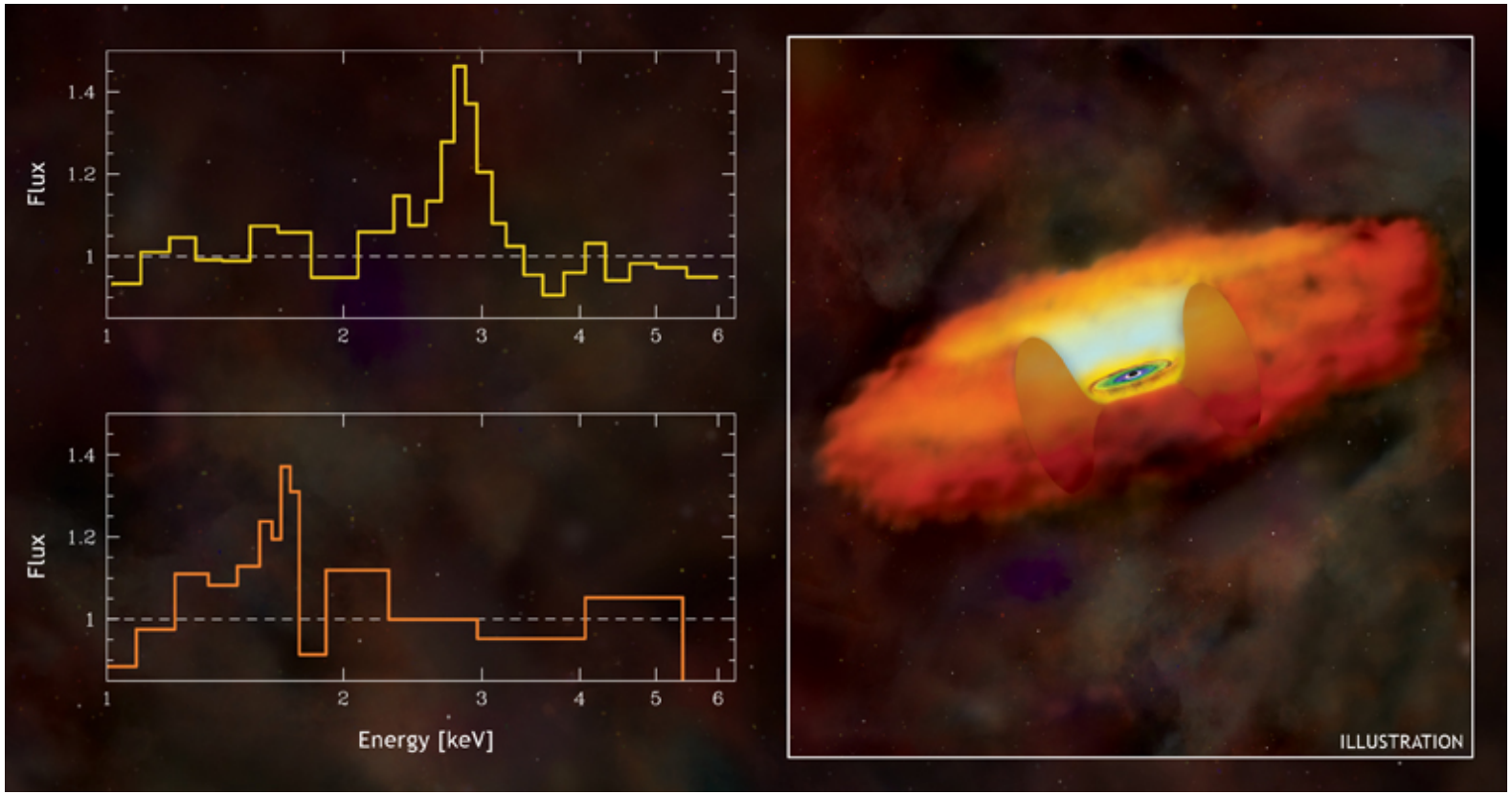


The left side of the above graphic shows portions of X-ray spectra from a subset of 50 black holes about 9 billion light years away (upper panel), and another group of 22 black holes that are about 11 billion light years away (lower panel).

# Chandra results

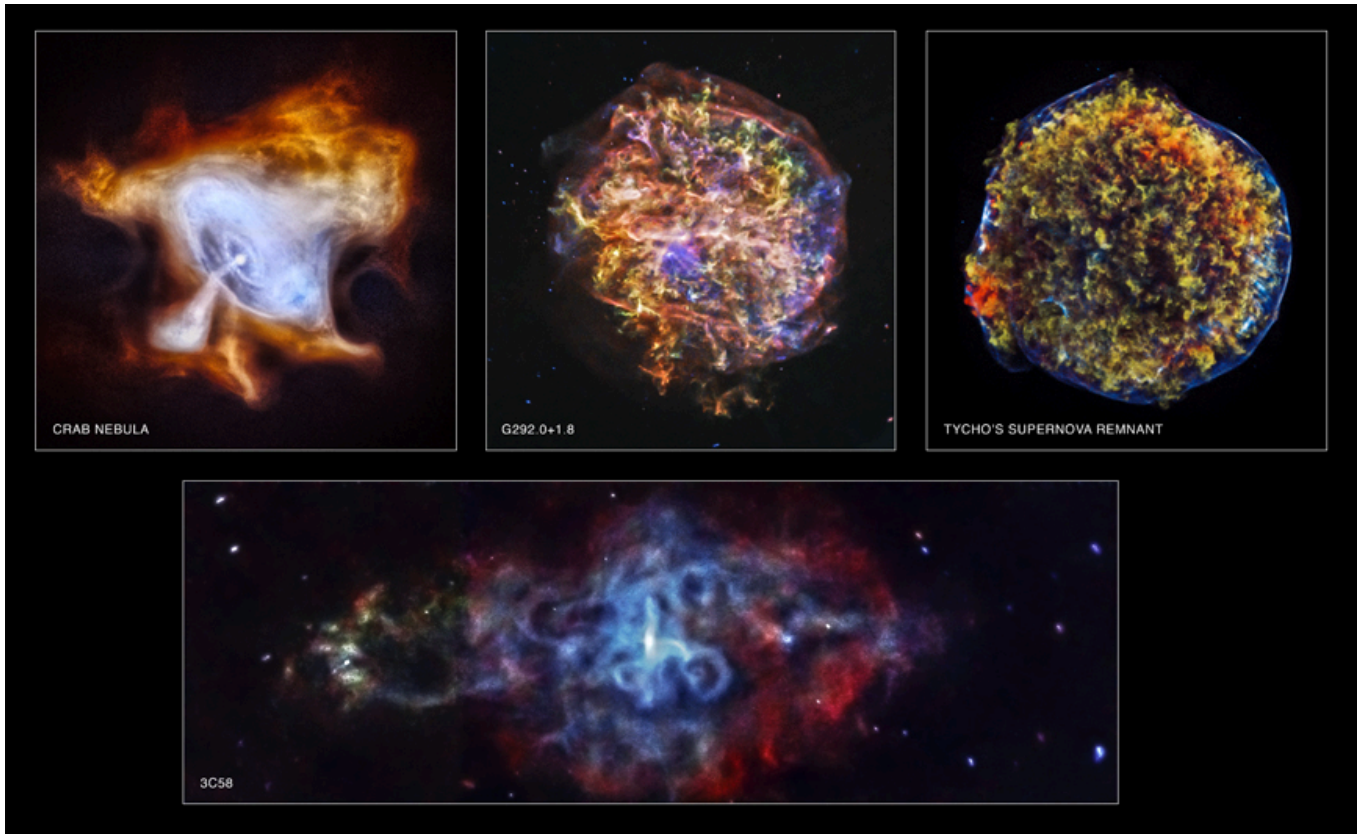


The Tycho and G292.0+1.8 supernova remnants show expanding debris from an exploded star and the associated shock waves.The images of the Crab Nebula and 3C58 show how neutron stars produced by a supernova can create clouds of high-energy particles.

# XMM results

- The XXL project, the largest XMM-Newton observing programme to date, set itself the ambitious task of mapping galaxy clusters back to a time when the Universe was just half of its present age. Its aim was to trace the evolution of the large-scale structure of the Universe.

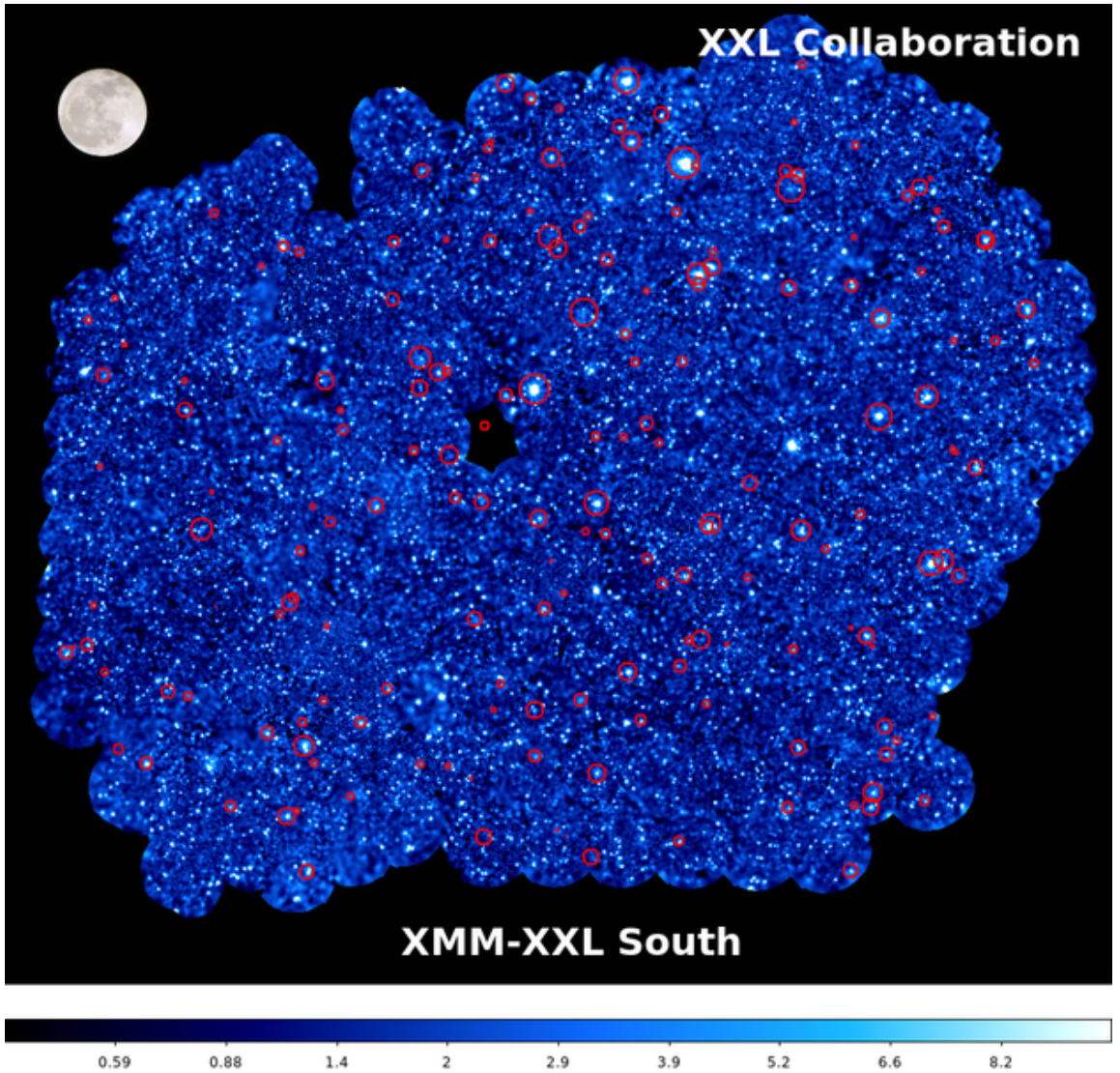

# XMM results

Components of the galaxy cluster Abell 2744, also known as the Pandora Cluster: galaxies (white), hot gas (red) and dark matter (blue).

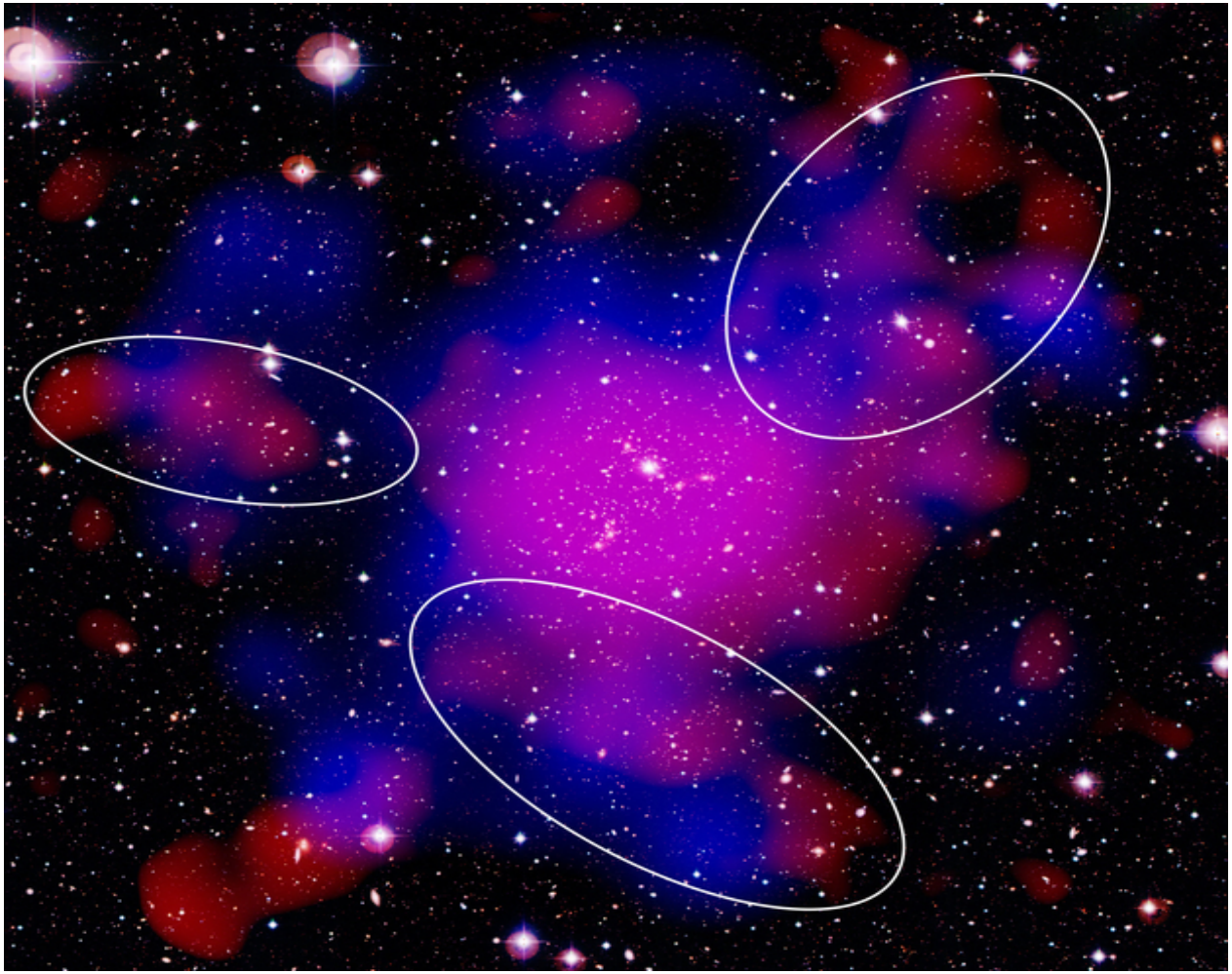

# X-ray science highlights

**Chandra Images by Category**


Solar System (9 listings)
Comets and planets


Normal Stars & Star Clusters (30 listings)
Stellar coronas, clusters of stars and hot gas produced by outflow from young stars.


White Dwarfs & Planetary Nebulas (10 listings)
Hot gas associated with the final stages of evolution of Sun-like stars, novas, and other white dwarfs in binary star systems.


Supernovas & Supernova Remnants (34 listings)
X-ray sources produced by the violent explosions of massive stars.


Neutron Stars/X-ray Binaries (26 listings)
Hot, isolated neutron stars, rotation-powered pulsars, and neutron stars accreting matter from a nearby companion star.


Black Holes (27 listings)
Stellar black holes, mid-mass black holes, and supermassive black holes.


Milky Way Galaxy (14 listings)
Images related to the Galactic Center and other features of the structure and evolution of the Milky Way Galaxy.


Normal Galaxies & Starburst Galaxies (39 listings)
Images of spiral, elliptical, and irregular galaxies that show X-ray sources associated with collapsed stars and star formation.


Quasars & Active Galaxies (33 listings)
Galaxies with unusually energetic activity, including high-energy jets, that is related to a central supermassive black hole.


Groups & Clusters of Galaxies (33 listings)
Vast clouds of hot gas embedded with numerous galaxies.


Cosmology/Deep Fields/X-ray Background (13 listings)
The sky as observed in X-rays is not dark, but gives off a glow thought to be from many distant sources. Deep surveys with the Chandra X-ray Observatory should reveal the cause of this glow.


Miscellaneous (8 listings)
Objects that don't fit in the above categories, such as brown dwarfs & gamma-ray bursts.

# X-ray science highlights

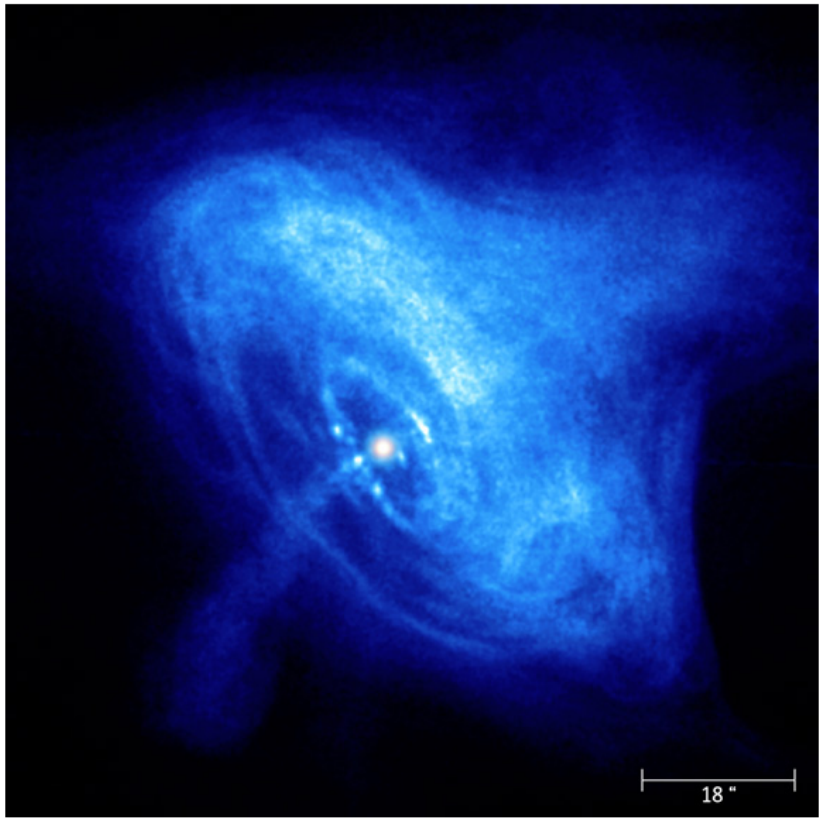


This image provides a view of the activity in the inner region around the Crab Nebula pulsar, a rapidly rotating neutron star seen as a bright white dot near the center of the images.

A wisp can be seen moving outward at half the speed of light from the upper right of the inner ring around the pulsar.
The wisp appears to merge with a larger outer ring that is visible in both X-ray and optical images.

The inner X-ray ring consists of about two dozen knots that form, brighten and fade. As a high-speed wind of matter and antimatter
particles from the pulsar plows into the surrounding nebula, it creates
a shock wave and forms the inner ring.
Energetic shocked particles move outward to
brighten the outer ring and produce an extended X-ray glow.

# X-ray science highlights

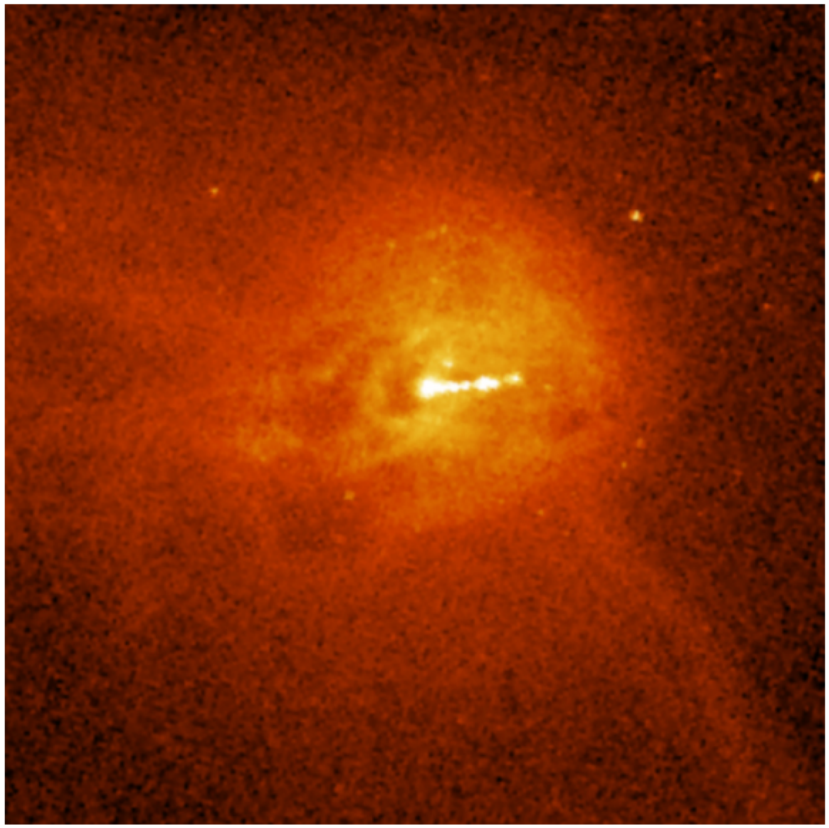

This close-up of M87 shows the region surrounding
the jet of high-energy particles in more detail.
The jet is thought to be pointed at a small angle to the
line of sight, out of the plane of the image.
This jet may be only the latest in a series of jets
that have been produced as magnetized
gas spirals in a disk toward the supermassive black hole

# X-ray science highlights

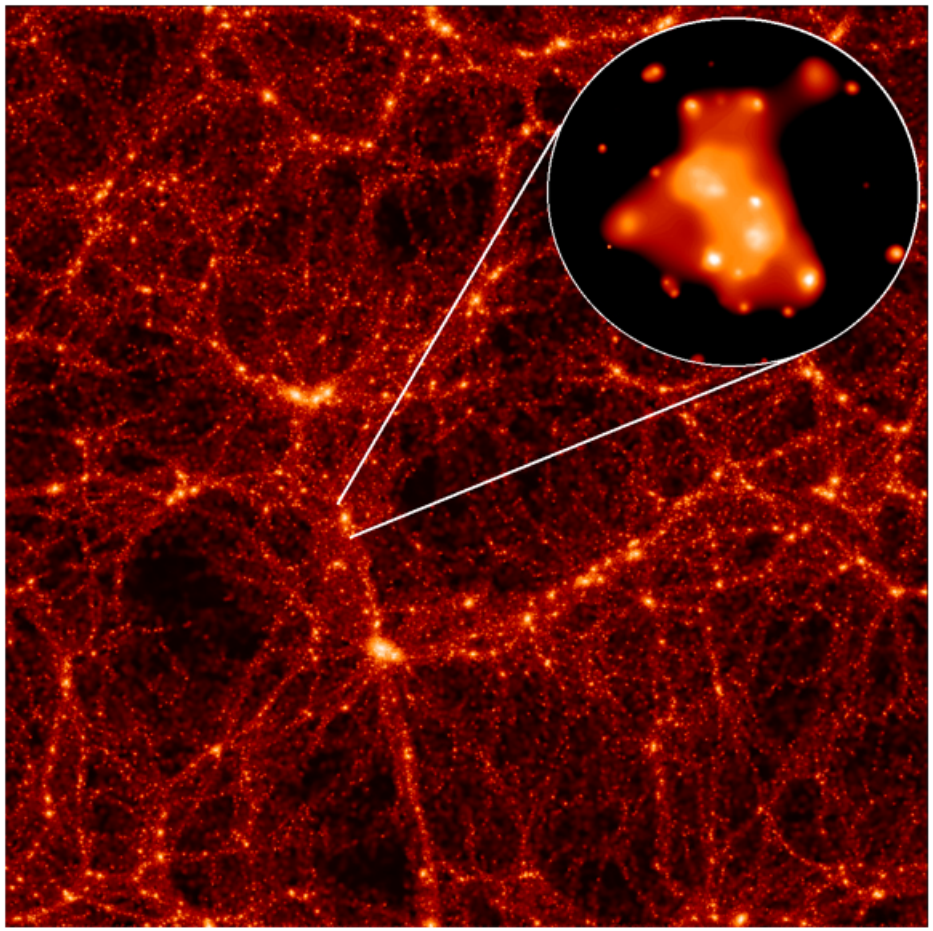

This image shows a computer simulation of a large volume of the Universe.
An XMM-Newton X-ray image of a real galaxy cluster from the study is superimposed to illustrate the formation of galaxy clusters in the densest parts of the universe.

# Dark Matter and Cosmo Simulations

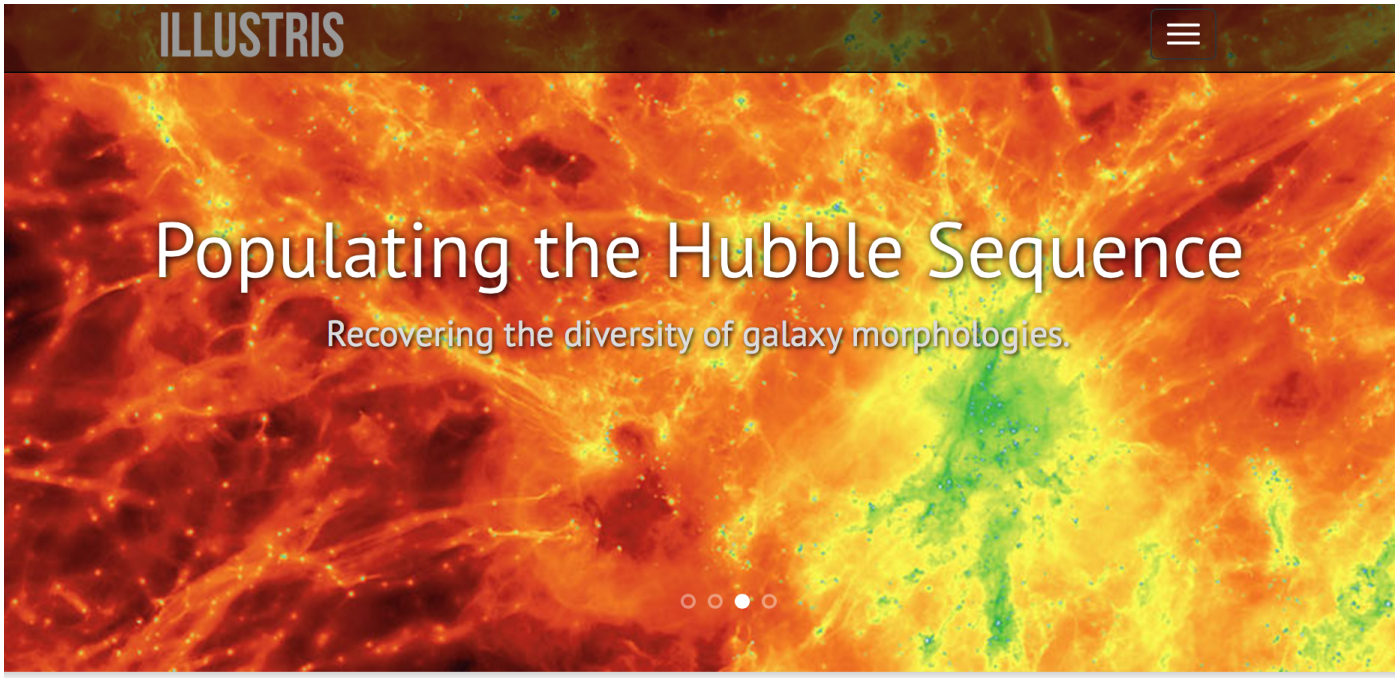


## Welcome

The Illustris project is a large cosmological simulation of galaxy formation, completed in late 2013, using a state of the art numerical code and a comprehensive physical model. Building on several years of effort by members of the collaboration, the Illustris simulation represents an unprecedented combination of high resolution, total volume, and physical fidelity. The About page contains detailed descriptions of the project, for both the general public and researchers in the field.

On this website we present the scientific motivation behind the project, a list of the collaboration members, key results and references, movies and images created from the simulation data, information on upcoming public data access, and tools for interactive data exploration. The short video below is a compilation made from some of the movies available on the Media page.

http://www.illustris-project.org



http://www.tng-project.org

# Dark Matter and Cosmo Simulations

## Numerical Simulations of the Dark Universe: State of the Art and the Next Decade

Michael Kuhlen[a], Mark Vogelsberger[b], Raul Angulo[c,d]

[a]*Theoretical Astrophysics Center, University of California Berkeley, Hearst Field Annex, Berkeley, CA 94720, USA*
[b]*Hubble Fellow, Harvard-Smithsonian Center for Astrophysics, 60 Garden Street, Cambridge, MA 02138, USA*
[c]*Max-Planck-Institute for Astrophysics, Karl-Schwarzschild-Str. 1, 85740 Garching, Germany*
[d]*Kavli Institute for Particle Astrophysics and Cosmology, Stanford University, Menlo Park, CA 94025, USA*

**Abstract**

We present a review of the current state of the art of cosmological dark matter simulations, with particular emphasis on the implications for dark matter detection efforts and studies of dark energy. This review is intended both for particle physicists, who may find the cosmological simulation literature opaque or confusing, and for astro-physicists, who may not be familiar with the role of simulations for observational and experimental probes of dark matter and dark energy. Our work is complementary to the contribution by M. Baldi in this issue, which focuses on the treatment of dark energy and cosmic acceleration in dedicated N-body simulations.

Truly massive dark matter-only simulations are being conducted on national supercomputing centers, employing from several billion to over half a trillion particles to simulate the formation and evolution of cosmologically representative volumes (cosmic scale) or to zoom in on individual halos (cluster and galactic scale). These simulations cost millions of core-hours, require tens to hundreds of terabytes of memory, and use up to petabytes of disk storage. Predictions from such simulations touch on almost every aspect of dark matter and dark energy studies, and we give a comprehensive overview of this connection. We also discuss the limitations of the cold and collisionless DM-only approach, and describe in some detail efforts to include different particle physics as well as baryonic physics in cosmological galaxy formation simulations, including a discussion of recent results highlighting how the distribution of dark matter in halos may be altered. We end with an outlook for the next decade, presenting our view of how the field can be expected to progress.

64

http://arxiv.org/pdf/1209.5745v2.pdf

# Suzaku

- Suzaku launched on July 10, 2005. Before launch it was called Astro-E2, and the name was changed to Suzaku shortly after the successful launch.
- Suzaku's four CCD cameras for low-energy X-rays and detector for high-energy X-rays continue to study the X-ray sky. In scientists' words, Suzaku is designed for "broad-band, high-sensitivity, high-resolution" spectroscopy.


http://www.isas.jaxa.jp/e/enterp/missions/suzaku/

# NuSTAR

- The NuSTAR (Nuclear Spectroscopic Telescope Array) mission has deployed the first orbiting telescopes to focus light in the high energy X-ray (3 - 79 keV) region of the electromagnetic spectrum. Our view of the universe in this spectral window has been limited because previous orbiting telescopes have not employed true focusing optics, but rather have used coded apertures that have intrinsically high backgrounds and limited sensitivity.

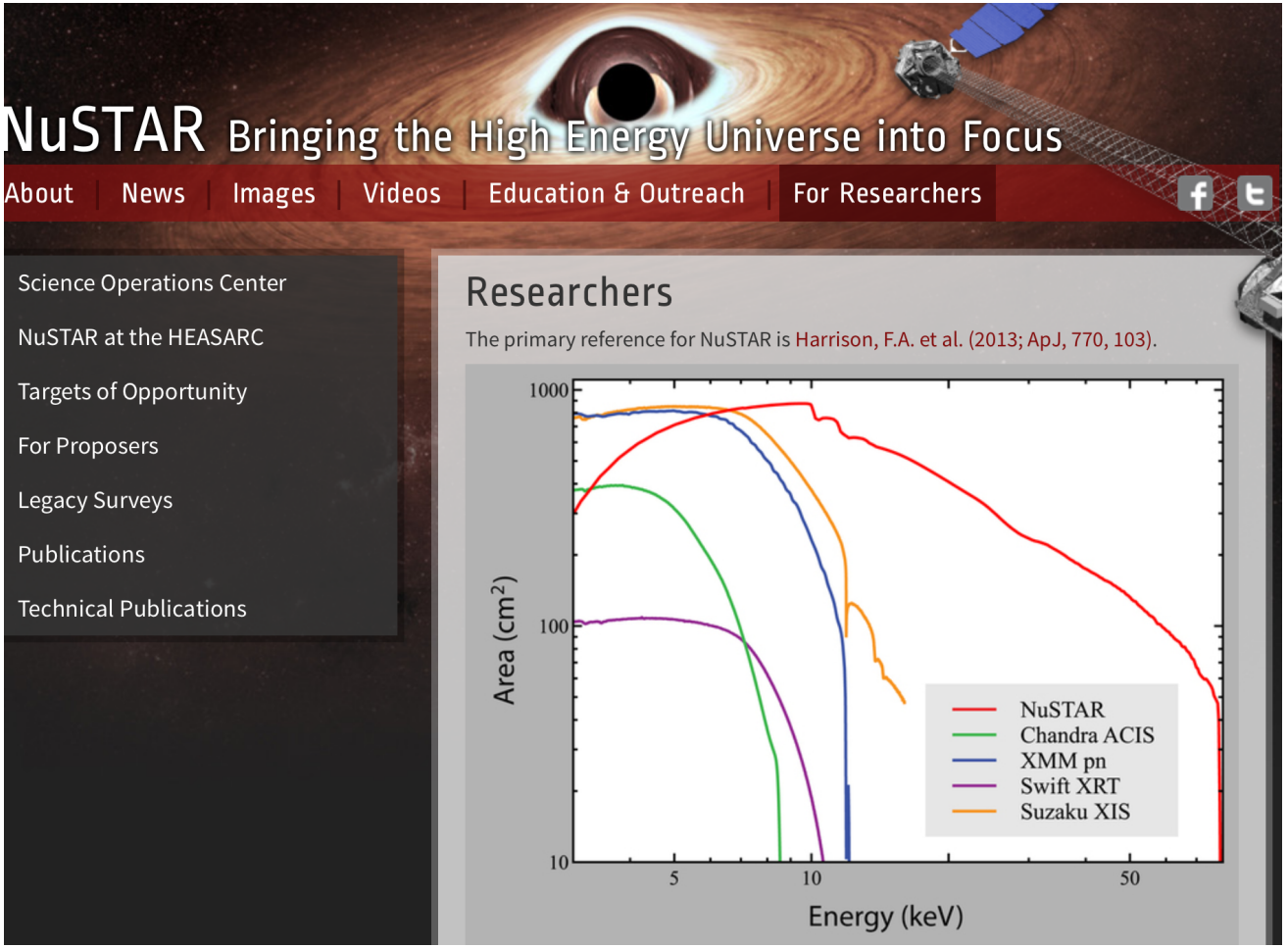


http://www.nustar.caltech.edu/

# MAXI

The Monitor of All-sky X-ray Image, MAXI, is the first experiment installed on the Japanese Experiment Module Exposed Facility (JEM-EF or Kibo-EF) on the International Space Station (ISS) and the first high energy astrophysical experiment placed on the space station.

The main objectives of MAXI are early detection of X-ray transient events, and monitoring the intensity fluctuation of known X-ray sources over long periods by scanning the all sky in soft and hard X-ray.

- two semi-circular arc-shaped X-ray slit cameras with wide FOVs. In the 92 minutes it takes the ISS to orbit the earch, MAXI gets a 360 deg image of the entire sky.
- two kinds of X-ray detectors, collecting events from the slit cameras: a gas proportional counters, the Gas Slit Camera (GSC; 2-30 keV), and a X-ray CCD, Solid-state Slit Camera (SSC; 0.5-12 keV).

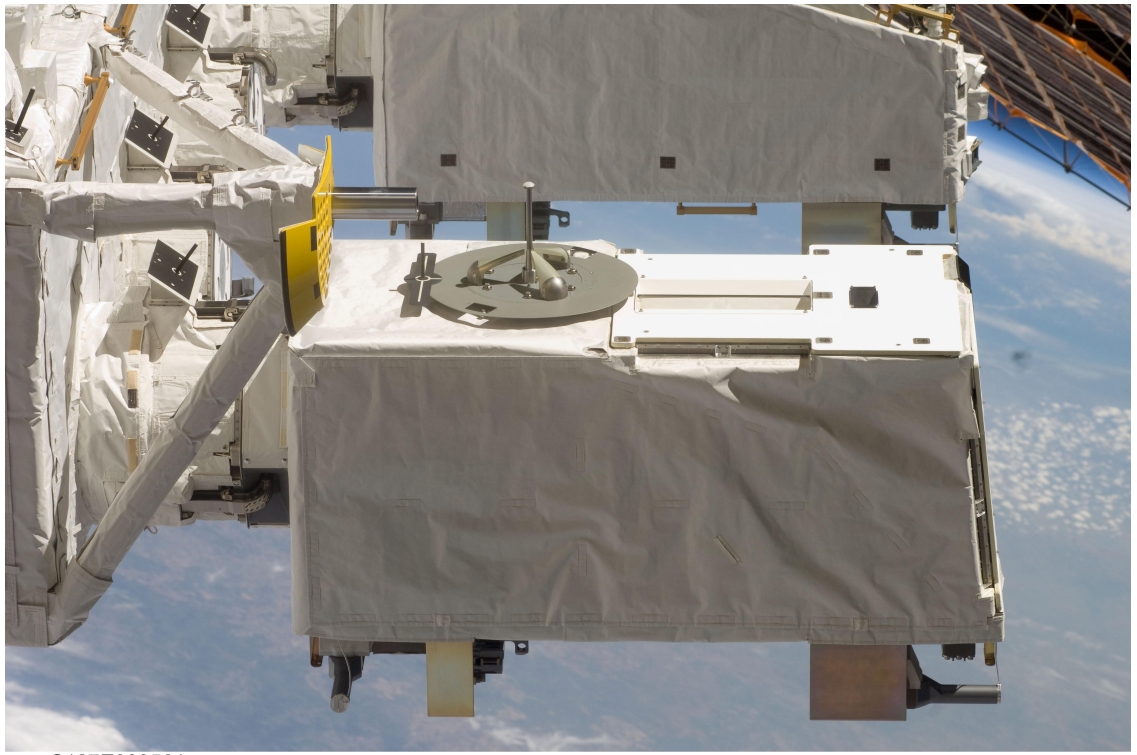

S127E009561

https://heasarc.gsfc.nasa.gov/docs/maxi/

# Astro-H – Hitomi

http://astro-h.isas.jaxa.jp/en/

# NICER

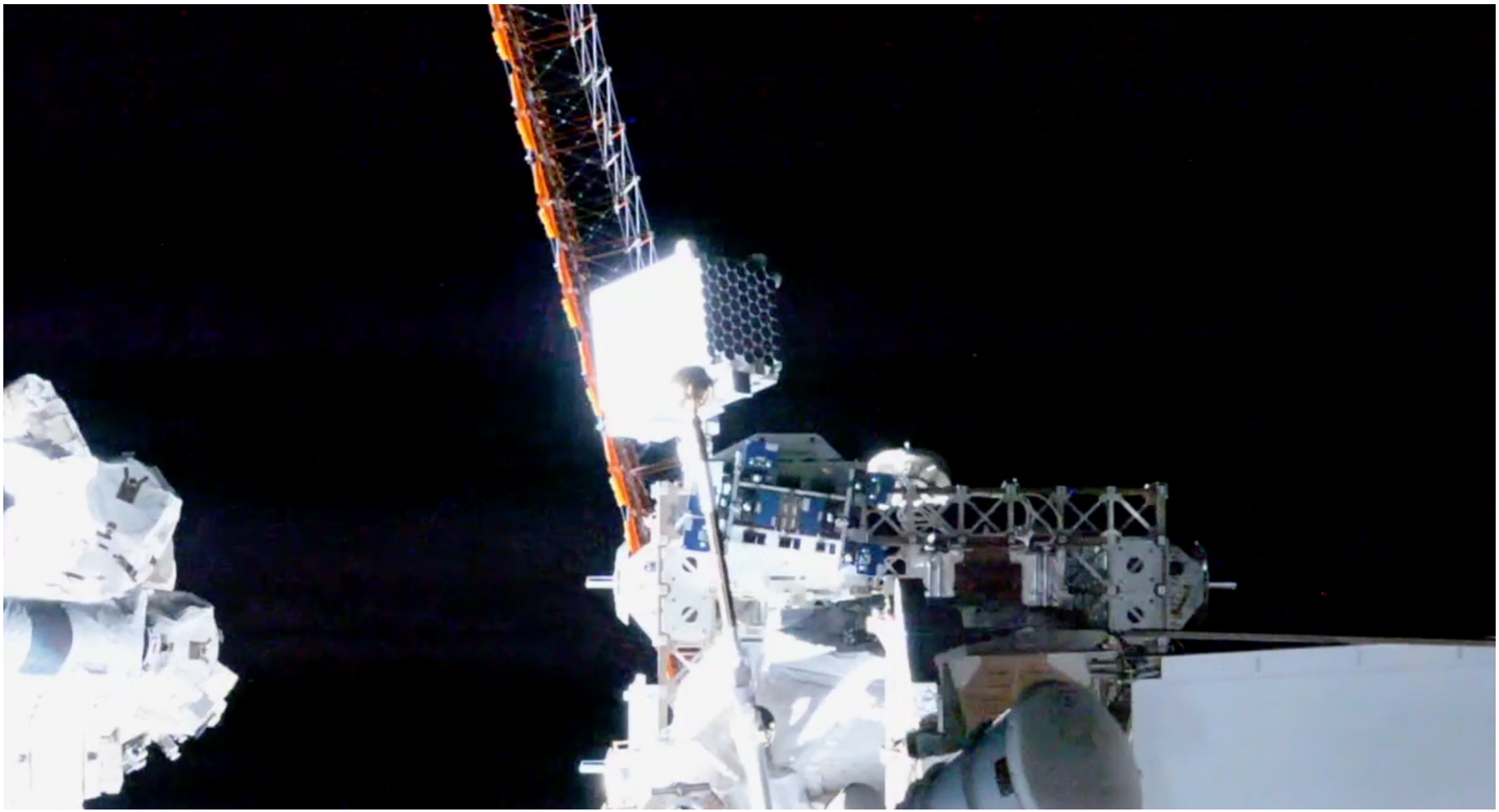

https://heasarc.gsfc.nasa.gov/docs/nicer/

# ASTROSAT

https://www.isro.gov.in/Spacecraft/astrosat

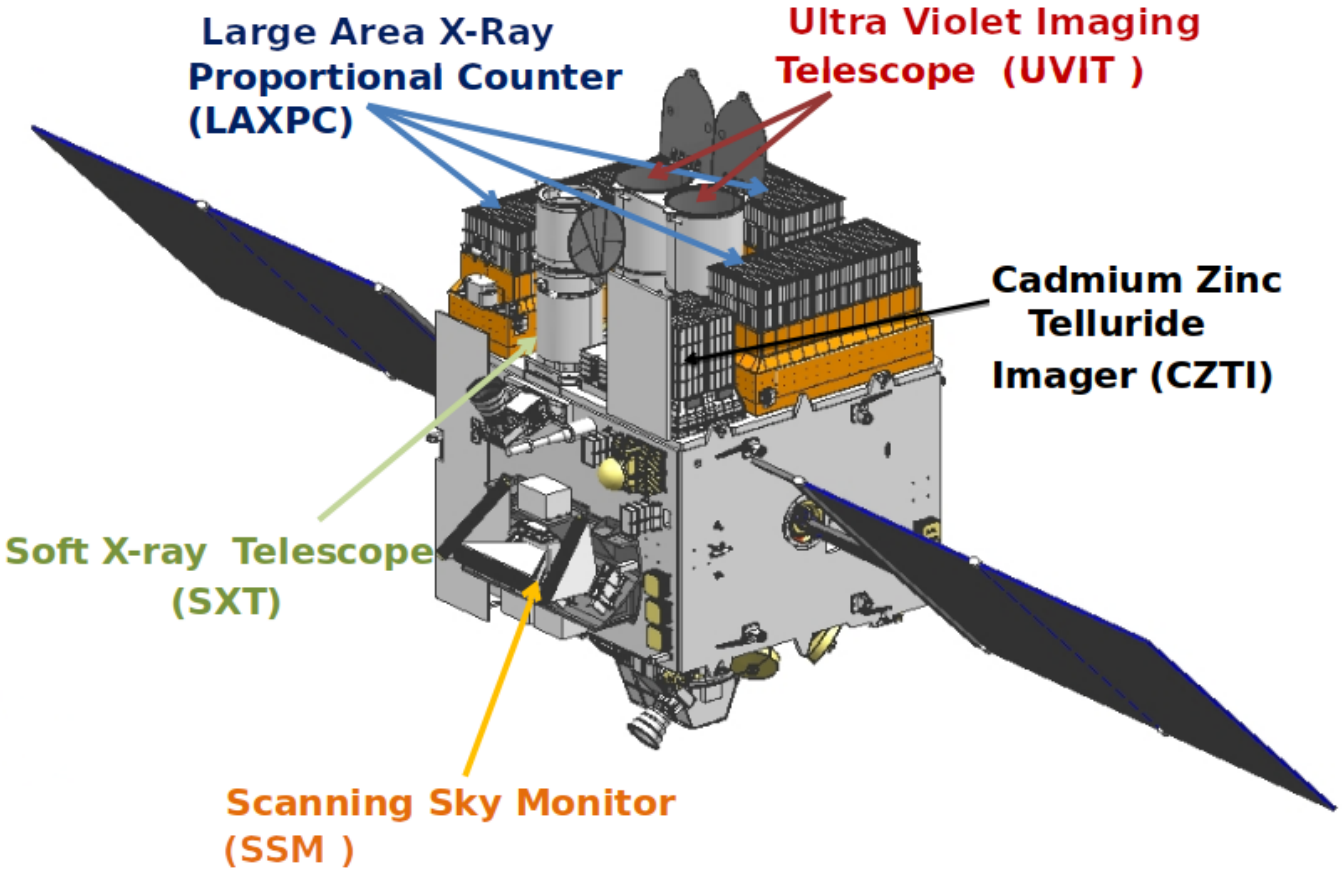


https://astrobrowse.issdc.gov.in/astro_archive/archive/Home.jsp

# HMXT

http://www.hxmt.org/index.php/enhome

# eROSITA

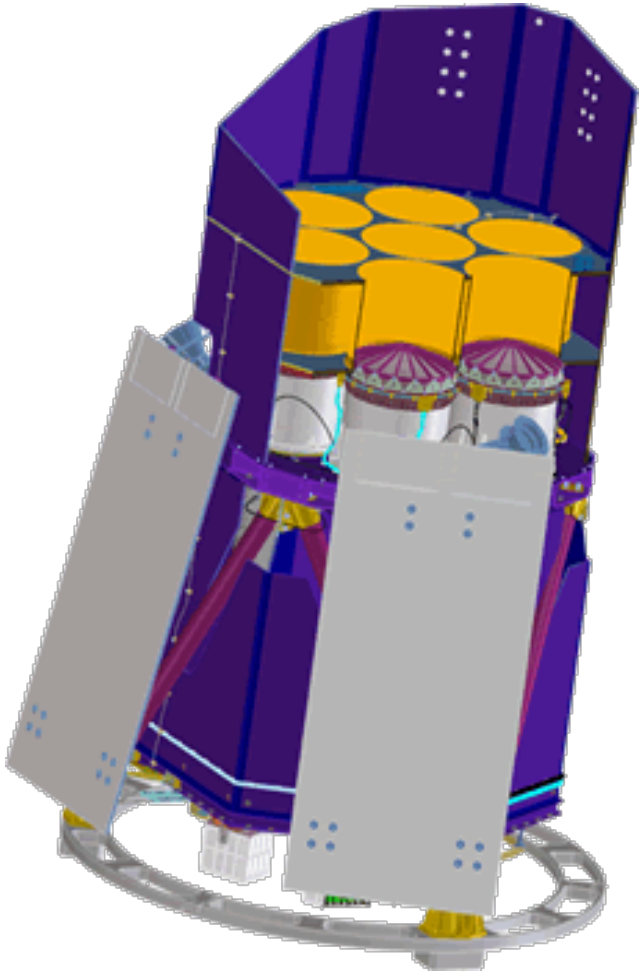

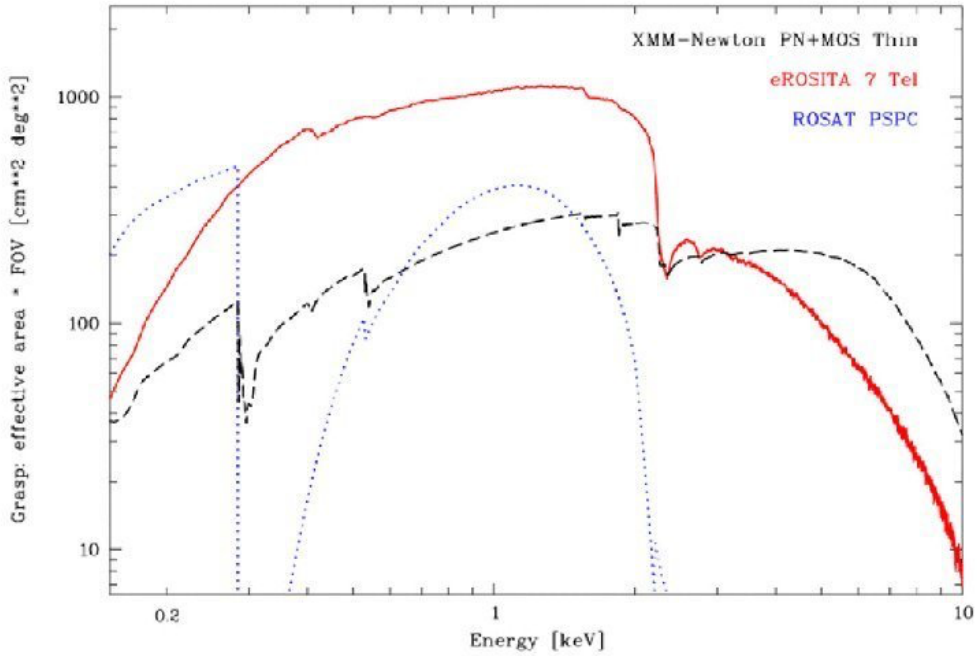


https://www.mpe.mpg.de/eROSITA

# XIPE

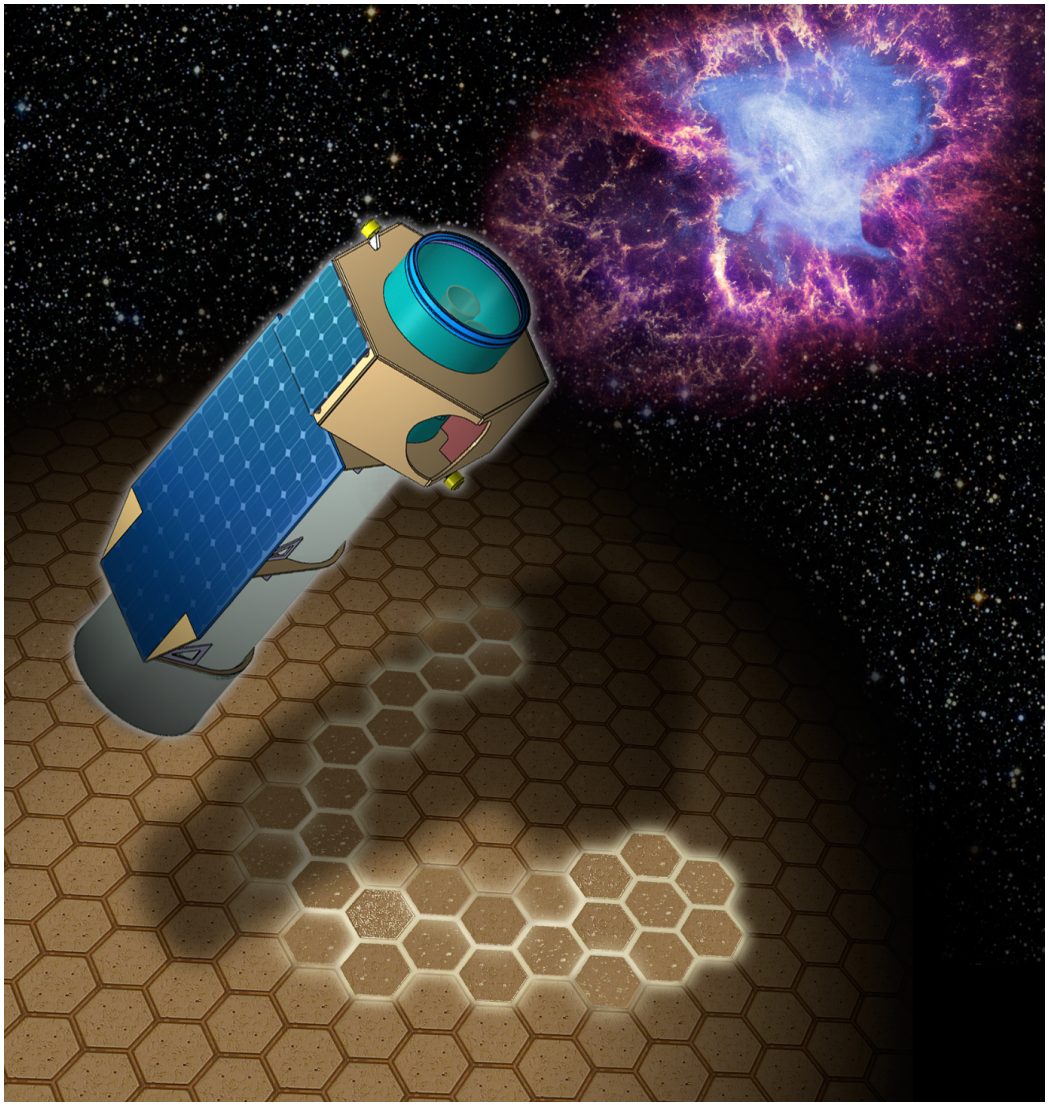

http://www.isdc.unige.ch/xipe/

# IXPE

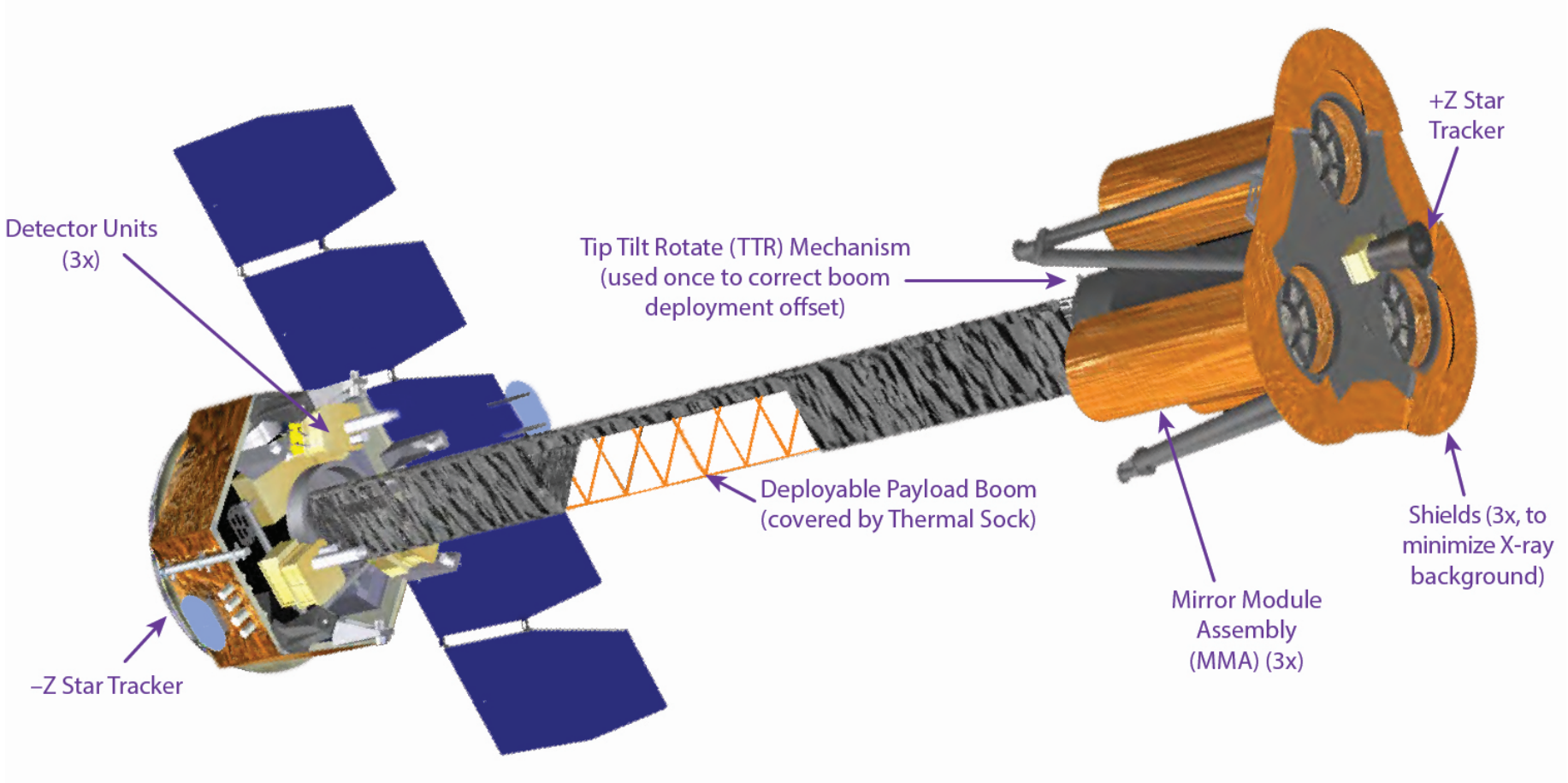


https://wwwastro.msfc.nasa.gov/ixpe/

# LOFT

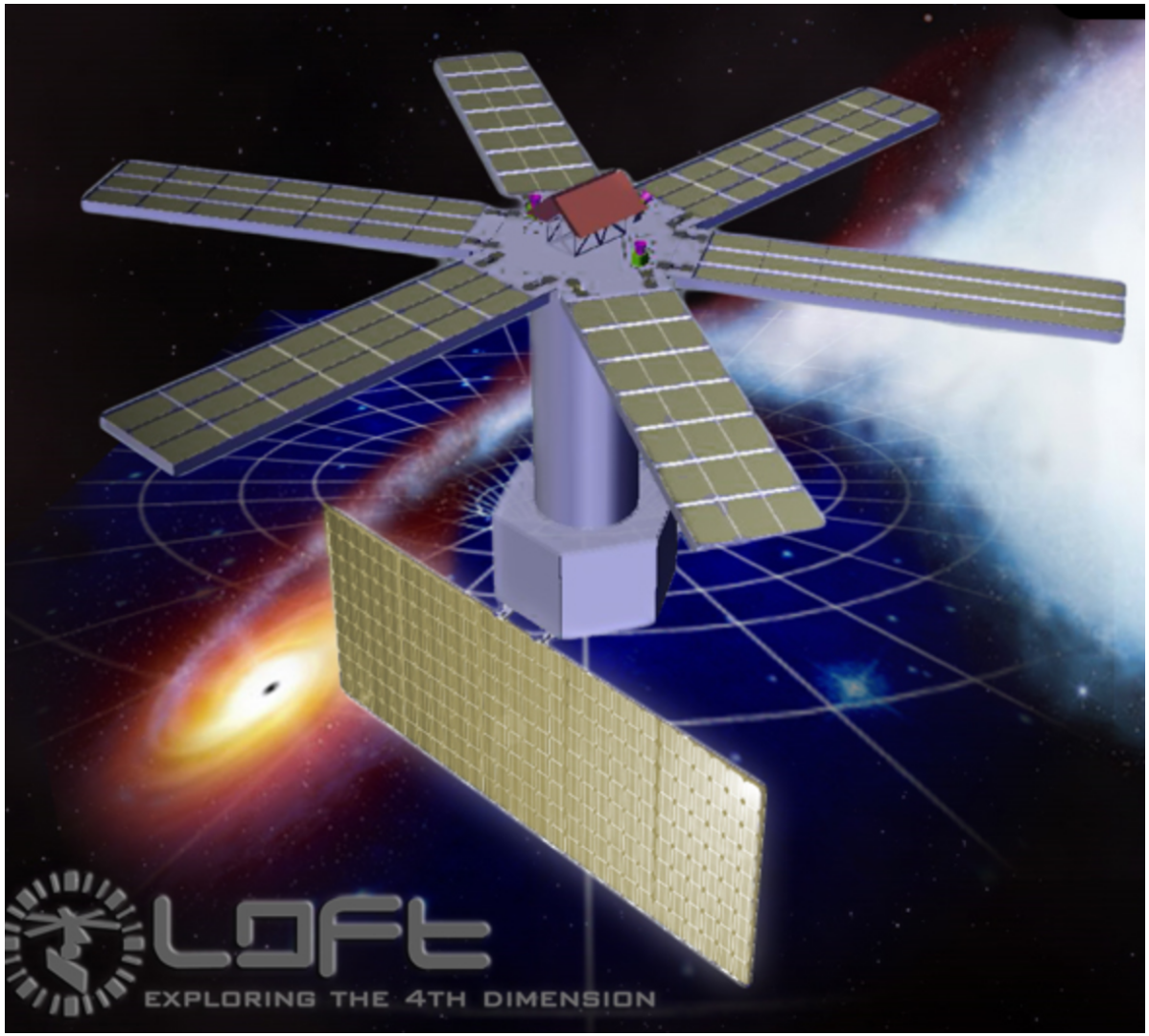


http://www.isdc.unige.ch/loft/

# eXTP

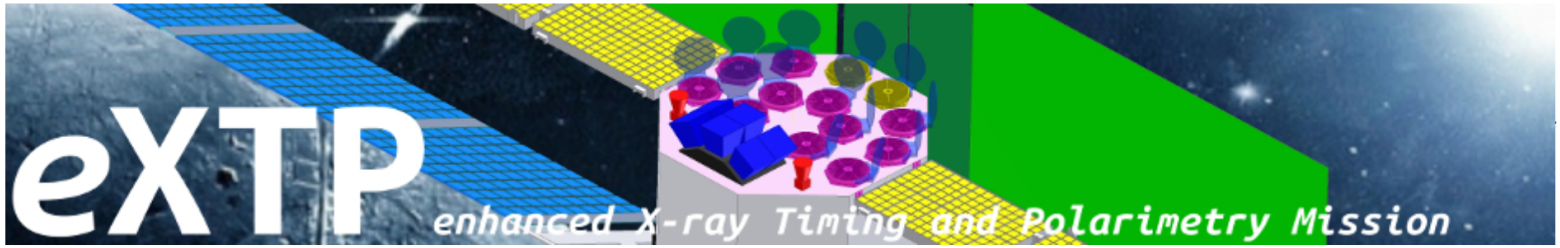


### The eXTP Mission



### eXTP Teams



### The eXTP Mission

The enhanced X-ray Timing and Polarimetry mission (eXTP) is a science mission designed to study the state of matter under extreme conditions of density, gravity and magnetism. Primary goals are the determination of the equation of state of matter at supra-nuclear density, the measurement of QED effects in highly magnetized star, and the study of accretion in the strong-field regime of gravity. Primary targets include isolated and binary neutron stars, strong magnetic field systems like magnetars, and stellar-mass and supermassive black holes.

The mission carries a unique and unprecedented suite of state-of-the-art scientific instruments enabling for the first time ever the simultaneous spectral-timing-polarimetry studies of cosmic sources in the energy range from 0.5-30 keV (and beyond). Key elements of the payload are:

- **the Spectroscopic Focusing Array** (**SFA**): a set of 11 X-ray optics operating in the 0.5-10 keV energy band with a field-of-view (FoV) of 12 arcmin each and a total effective area of ~0.9 $m^2$ and 0.6 $m^2$ at 2 keV and 6 keV respectively. The telescopes are equipped with Silicon Drift Detectors offering <180 eV spectral resolution.
- **the Large Area Detector** (**LAD**): a deployable set of 640 Silicon Drift Detectors, achieving a total effective area of ~3.4 $m^2$ between 6 and 10 keV. The operational energy range is 2-30 keV and the achievable spectral resolution better than 250 eV. This is a non-imaging instrument, with the FoV limited to <1° FWHM by the usage of compact capillary plates.
- **the Polarimetry Focusing Array** (**PFA**): a set of 2 X-ray telescope, achieving a total effective area of 250 $cm^2$ at 2 keV, equipped with imaging gas pixel photoelectric polarimeters. The FoV of each telescope is 12 arcmin and the operating energy range is 2-10 keV.
- **the Wide Field Monitor** (**WFM**): a set of 3 coded mask wide field units, equipped with position-sensitive Silicon Drift Detectors, covering in total a FoV of 3.7 sr and operating in the energy range 2-50 keV.

http://www.isdc.unige.ch/extp/

# Athena

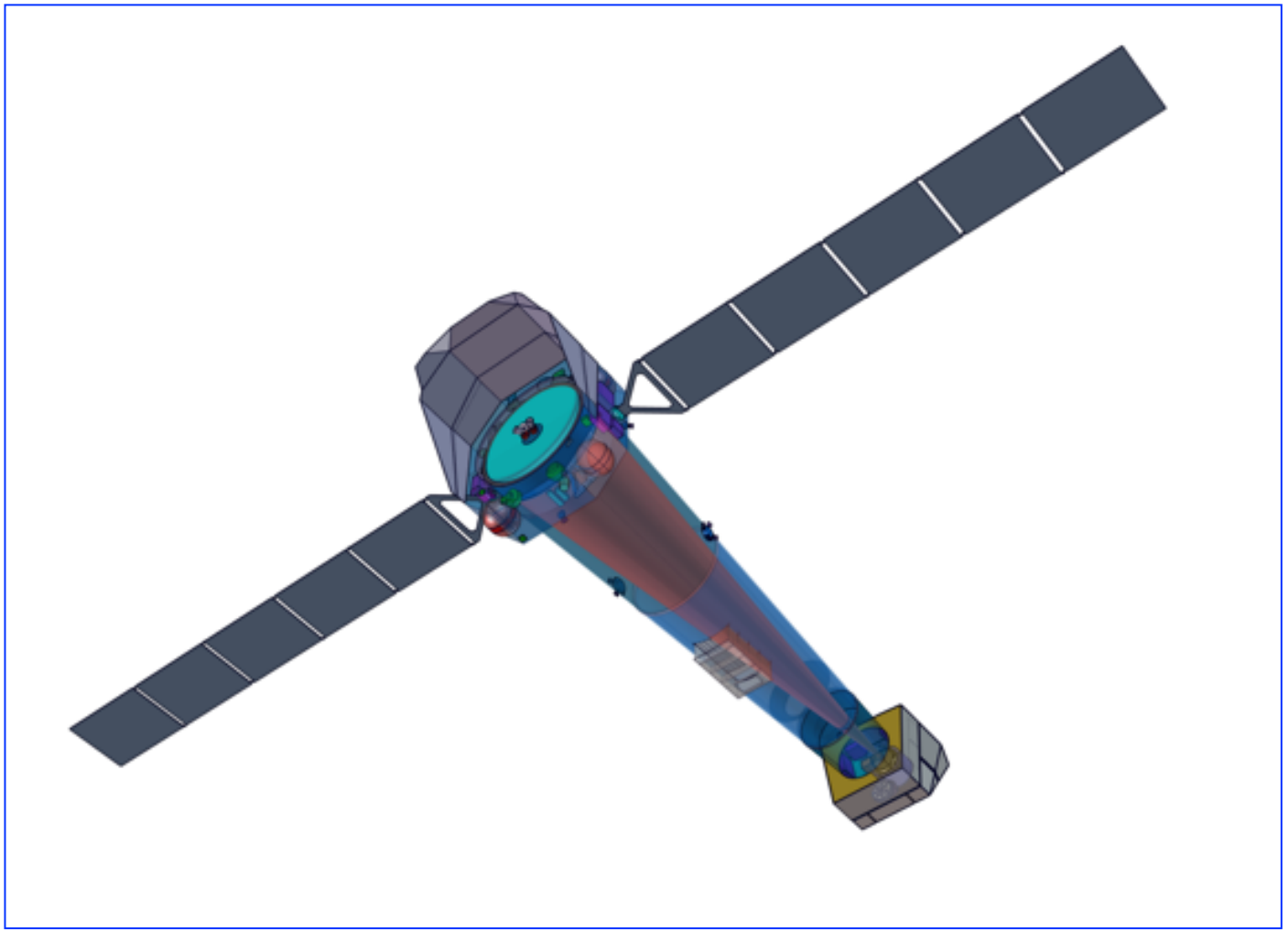

https://www.the-athena-x-ray-observatory.eu